Neuropharmacology 97 (2015) 289–305

Contents lists available at ScienceDirect

Neuropharmacology

journal homepage: www.elsevier.com/locate/neuropharm

Oxaliplatin-induced neurotoxicity is mediated through gap junction channels and hemichannels and can be prevented by octanol

Alexia Kagiava [a], George Theophilidis [c], Irene Sargiannidou [a], Kyriacos Kyriacou [d], Kleopas A. Kleopa [a, b, *]

[a] Neuroscience Laboratory, The Cyprus Institute of Neurology and Genetics, Cyprus School of Molecular Medicine, Nicosia, Cyprus
[b] Neurology Clinics, The Cyprus Institute of Neurology and Genetics, Cyprus School of Molecular Medicine, Nicosia, Cyprus
[c] Laboratory of Animal Physiology, Department of Zoology, School of Biology, Aristotle University of Thessaloniki, Thessaloniki, Greece
[d] Department of Molecular Pathology and Electron Microscopy, The Cyprus Institute of Neurology and Genetics, Cyprus School of Molecular Medicine, Nicosia, Cyprus

ARTICLE INFO

Article history:
Received 30 October 2014
Received in revised form
16 April 2015
Accepted 16 May 2015
Available online 1 June 2015

Keywords:
Chemotherapy-induced neuropathy
Gap junctions
Action potential
Cx32
Cx29
Juxtaparanodes
Sciatic nerve

ABSTRACT

Oxaliplatin-induced neurotoxicity (OIN) is a common complication of chemotherapy without effective treatment. In order to clarify the mechanisms of both acute and chronic OIN, we used an *ex-vivo* mouse sciatic nerve model. Exposure to 25 μM oxaliplatin caused a marked prolongation in the duration of the nerve evoked compound action potential (CAP) by nearly 1200% within 300 min while amplitude remained constant for over 20 h. This oxaliplatin effect was almost completely reversed by the gap junction (GJ) inhibitor octanol in a concentration-dependent manner. Further GJ blockers showed similar effects although with a narrower therapeutic window. To clarify the target molecule we studied sciatic nerves from connexin32 (Cx32) and Cx29 knockout (KO) mice. The oxaliplatin effect and neuroprotection by octanol partially persisted in Cx29 better than in Cx32 KO nerves, suggesting that oxaliplatin affects both, but Cx32 GJ channels more than Cx29 hemichannels. Oxaliplatin also accelerated neurobiotin uptake in HeLa cells expressing the human ortholog of Cx29, Cx31.3, as well as dye transfer between cells expressing the human Cx32, and this effect was blocked by octanol. Oxaliplatin caused no morphological changes initially (up to 3 h of exposure), but prolonged nerve exposure caused juxtaparonodal axonal edema, which was prevented by octanol. Our study indicates that oxaliplatin causes forced opening of Cx32 channels and Cx29 hemichannels in peripheral myelinated fibers leading to disruption of axonal K^+ homeostasis. The GJ blocker octanol prevents OIN at very low concentrations and should be further studied as a neuroprotectant.

1. Introduction

Oxaliplatin is used extensively as a first-line drug in gastrointestinal cancer chemotherapy, in particular metastatic colorectal cancer (Andre et al., 2004). The major dose-limiting toxicity of oxaliplatin is peripheral neuropathy that can manifest in over 60% of treated patients. Oxaliplatin-induced neurotoxicity (OIN) can present both as an acute or as chronic neuropathy. Acute OIN manifestations are characterized by peripheral nerve hyperexcitability symptoms, including cold-induced perioral or pharyngolaryngeal dysesthesias (Kweekel et al., 2005; Park et al., 2009). The origin of OIN and hyperexcitability symptoms remains controversial, although a variety of mechanisms have been proposed. Several studies implicated the involvement of voltage-gated potassium channels (VGKCs) (Benoit et al., 2006; Kagiava et al., 2008; Lang et al., 2008; Sittl et al., 2010; Nodera et al., 2011; Dimitrov and Dimitrova, 2012; Kagiava et al., 2013), others focused on voltage-gated sodium channels (VGNaCs) (Adelsberger et al., 2000; Webster et al., 2005; Krishnan et al., 2006; Park et al., 2011; Argyriou et al., 2013) and some attributed OIN to oxalate, a well-known chelator of both intracellular calcium and magnesium, that is liberated by oxaliplatin (Grolleau et al., 2001; Hochster et al., 2007; Sakurai et al., 2009; Tatsushima et al., 2013). However, none of the proposed mechanisms has so far provided a definite solution to understanding the pathogenesis of OIN as a basis for offering effective prevention and treatment

* Corresponding author. Neuroscience Laboratory, The Cyprus Institute of Neurology and Genetics, 6 International Airport Avenue, P.O. Box 23462, 1683, Nicosia, Cyprus. Tel.: +357 22 358600; fax: +357 22 392786.
E-mail address: kleopa@cing.ac.cy (K.A. Kleopa).

http://dx.doi.org/10.1016/j.neuropharm.2015.05.021
0028-3908/

(Wilson et al., 2002; von Delius et al., 2007; Broomand et al., 2009; Ferrier et al., 2013; Loprinzi et al., 2014).

Our previous *ex vivo* studies on the isolated rat sciatic nerve exposed to oxaliplatin suggested that the physiological correlate of OIN is a form of a post-stimulus severe broadening of the repolarising phase of the evoked nerve compound action potential (CAP), called here the "oxaliplatin-effect", which developed in a concentration- and time-dependent manner (Kagiava et al., 2008). Moreover, in the same nerve preparation, intra-axonal recordings from nerve fibers exposed to oxaliplatin have shown that hyperexcitability occurs either as a repetitive firing, or as a 400% broadening of the repolarising phase of the CAP, while the resting membrane potential of the axon remains unaffected (Kagiava et al., 2013). Such an effect is unique in the pharmacology of the adult mammalian axons and has been shown only once in intra-axonal recordings from nerve fibers of young rats, with relatively thin myelin, treated with 4-aminopyridine (4-AP), a well-known VGKC blocker (Kocsis et al., 1987). However, 4-AP or tetraethylammonium (TEA) had no effect on adult myelinated nerve fibers (Kagiava et al., 2008).

Despite our previous *ex vivo* studies and reports from several other laboratories indicating that VGKCs dysfunction could play a role in OIN, VGKCs are unlikely to be the primary target because patch-clamp studies failed to show any binding of oxaliplatin on *Shaker*-type Kv1.1/1.2 (Broomand et al., 2009). Since these VGKCs are responsible for the repolarizing phase of the action potential (Kocsis et al., 1987; Chiu, 1991; Zhou et al., 1999), which is drastically affected by oxaliplatin, we hypothesized that oxaliplatin may affect a functionally closely related target, leading indirectly to VGKC dysfunction. Particularly relevant as potential targets appear to be the gap junction (GJ) channels and hemichannels in the myelin sheath, which are thought to play a crucial role in the removal of excess K^+ from the periaxonal space through the myelin layers. Hemichannels formed by connexin29 (Cx29, the human ortholog is Cx31.3) at the innermost myelin membrane surrounding the juxtaparanodal regions, directly appose axonal VGKCs and likely participate in the regulation of K^+ during the generation of an action potential (Altevogt et al., 2002; Sargiannidou et al., 2008). Due to this striking proximity to Kv1.1/1.2 VGKCs, Cx29 hemichannels have been proposed to open and allow the transport into Schwann cell cytoplasm of surplus K^+ released from the axonal juxtaparanodal region during the action potential that would otherwise accumulate in the periaxonal space (Konishi, 1990; Chiu, 1991; Altevogt et al., 2002). Since Cx29 hemichannels are only found in the innermost myelin layers, this functional pathway for the regulation of K^+ likely also involves Cx32 GJ channels that provide a passage through the entire myelin sheath reaching the abaxonal Schwann cell cytoplasm (Scherer et al., 1995; Balice-Gordon et al., 1998; Kleopa, 2011).

The proposed role of Cx29 hemichannels and Cx32 GJ channels functioning together to provide a mechanism for preserving the homeostasis of K^+ ions suggests that they may be involved in OIN as well. It has already been shown that the action of oxaliplatin occurs only in myelinated fibers, since oxaliplatin induced bursts of action potentials in myelinated A-fibers, but not in unmyelinated C-fibers (Sittl et al., 2010). Additionally, recent studies have shown that oxaliplatin can affect the expression levels of GJs in astrocytes (Yoon et al., 2013) and dorsal root ganglia (DRG) satellite glial cells (Warwick and Hanani, 2013), while GJ blockage by carbenoxolone results in analgesic-like effects (Rouach et al., 2003; Vessey et al., 2004). Furthermore, GJ hemichannel blockade was found to be neuroprotective in some cases of global cerebral ischemia in near-term fetal sheep (Davidson et al., 2014), while gap junctional communication could counteract the effects of the anti-tumor agent cisplatin (homologous to oxaliplatin) (Broomand et al., 2009). Recent studies of taxol and oxaliplatin neurotoxicity suggested that GJ blockers may have potential in treating chemotherapy-induced neuropathic pain (Warwick and Hanani, 2013). However, none of these studies has focused on connexins expressed in peripheral myelinated fibers, where oxaliplatin causes most pathological changes (Burakgazi et al., 2011; Krøigård et al., 2014).

Here, we report the detailed electrophysiological and morphological correlates of OIN in the *ex vivo* sciatic nerve preparation and provide evidence that OIN is mediated by Cx32 GJ channels and Cx29/Cx31.3 GJ hemichannels in myelinated fibers. Moreover, we demonstrate that octanol, a GJ blocker, can prevent both the functional and the morphological changes induced by oxaliplatin *ex vivo* and *in vitro*.

2. Methods

2.1. Mouse strains and procedures

We used two month old wild type (WT) C57BL/6, as well as *Gjb1*-null mice/Cx32 knockout (KO) (C57BL/6_129) and *Gjc3*-null/Cx29 KO (129P2/OlaHsd*C57BL/6*SJL) mice weighing 20–25 g, which were obtained from the European Mouse Mutant Archive (Monterotondo, Italy), both originally generated by Prof. Klaus Willecke (University of Bonn, Bonn, Germany). Animals were sacrificed using N_2 and cervical dislocation prior to nerve dissection. The sciatic nerve was exposed and dissected from the spinal cord to the knee. All experimental procedures were conducted in accordance with the animal care protocols outlined by the Aristotle University of Thessaloniki, Greece and the Veterinary Authorities (License No 107241/2013) and the Cyprus Government's Chief Veterinary Officer according to EU guidelines (EC Directive 86/609/EEC).

2.2. Ex vivo sciatic nerve recording bath

The sciatic nerves were immersed in a modified Krebs–Ringer solution containing (in mmol/l): 136 NaCl, 4.7 KCl, 2.4 $CaCl_2$, 1.1 $MgCl_2$, 1 $NaHCO_3$, 11 glucose, and 10 HEPES (all from Sigma, Germany); pH = 7.2. All experiments were performed at a constant temperature of 25.0 ± 1.0 °C. The epineural sheath was removed to ensure that nerve fibers came into direct contact with the drug under investigation and to maximize drug access to all nerve fibers. To expose the nerve to the drug under investigation and simultaneously monitor its electrophysiological responses to electrical stimuli (whole-nerve extracellular recordings), we used a three-chambered recording bath made of paraffin as described in detail in our previous studies (Kagiava et al., 2012). A similar, though slightly larger, recording bath, has been used for a variety of neurotoxicological studies on the rat sciatic nerve (Kagiava et al., 2008, 2013). Briefly, the recording bath consists of three chambers: the stimulating, the perfusion (middle), and the recording chamber. The chambers with volume of 10–11 ml were placed in a row 1 mm apart. The nerve was mounted across the three chambers of the recording bath with 2–3 mm of the proximal part of the nerve placed in the stimulating chamber, where it was electrically stimulated with supramaximal stimuli at 1 Hz (pulse amplitude: 2.0–3.0 V, duration: 0.01 ms) using an electrode connected to a constant voltage stimulator (Digitimer, England, UK) to evoke the CAP. The main region of the nerve – about 10–12 mm, over 70.0% of the total nerve length – was bathed in the perfusion chamber and was exposed to the saline (control) or the drugs under investigation (oxaliplatin, octanol and their combination). Finally, the distal part of the nerve was placed in the recording chamber, where the evoked CAP was recorded using an electrode immersed in the chamber connected to AC amplifier (Neurolog NL822, Digitimer, UK). Immediately after the placement of the nerve, each chamber was filled once with 10.0 ml oxygenated (O_2, 100%) saline. During the 24 h recording period the saline in the perfusion chamber was continuously stirred using a miniature magnet and pH remained stable. The electrodes (active and reference) from either amplifier or stimulator were made of 24-carat gold. Finally, the recording bath was air-tight shielded to avoid evaporation of the saline during the long recording period (>20 h).

2.3. Electrophysiological data analysis

The amplitude of the CAP (example of baseline recorded evoked CAPs is given in Fig. 1A) was measured from the baseline to the peak (in Volts). The duration of the repolarizing phase of the CAP or the repolarizing time (RT) was measured from the peak up to the end of the repolarizing phase (in ms), at the point where the repolarizing phase meets the baseline (example in Fig. 2A). CAP amplitude and RT measured in Volts and ms, respectively, were expressed as a percentage of the initial values at t = 0, or of the values before the application of the tested compound, which were considered as 100%. Values obtained from repeated experiments were averaged and expressed as means ± SEM. Using these values, the mean time-response curves were plotted (example in Fig. 1E). Statistical significance was examined by one-way ANOVA and Student's t-test.

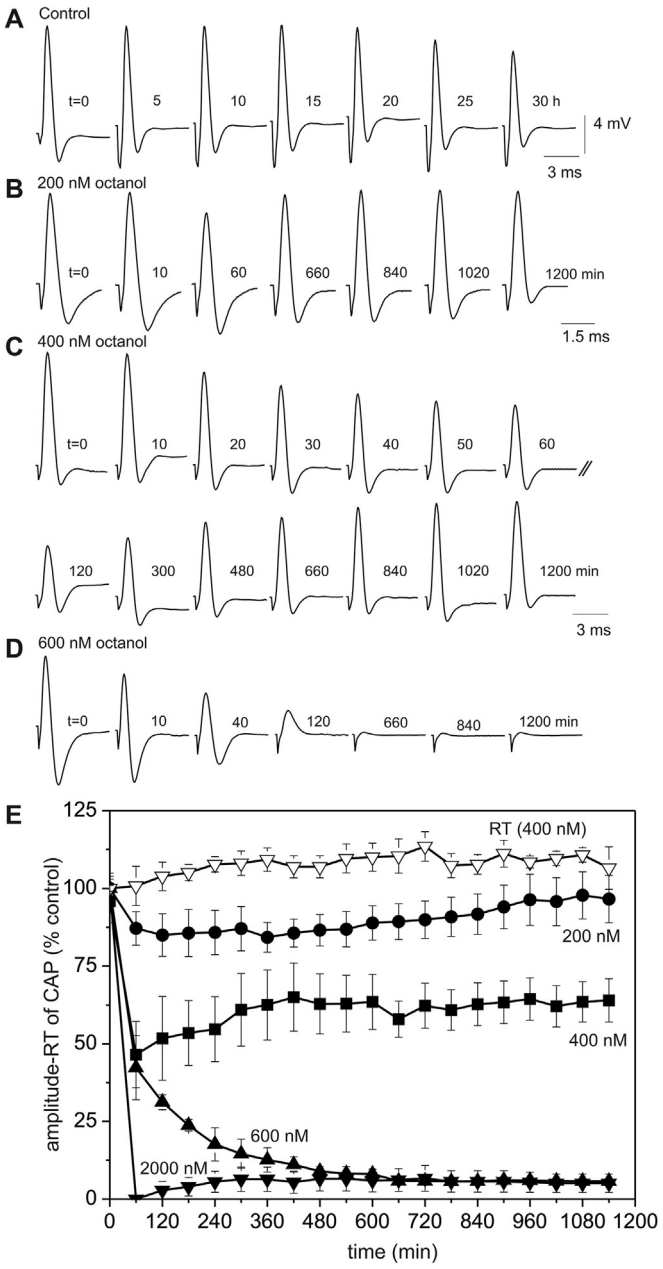

Fig. 1. The effects of octanol on mouse sciatic nerve isolated in the three-chamber recording bath. (A) Recordings of the evoked CAP from a control nerve immersed in normal saline. The time point of each CAP recording is indicated by (t). (B–D) show representative recordings from nerves immersed in octanol 200 (B), 400 (C) and 600 nM (D). (E) Mean time-response curves (average of n = 4–6 experiments) showing the percentage decrease in the amplitude of the evoked CAP as a function of incubation time in octanol 200, 400, 600 and 2000 nM, as indicated. The amplitude of the evoked CAP at time 0, before the application of octanol, was considered to be 100%. The curve marked with the open triangles represents the mean time-response curve for the repolarising time (RT) of the evoked CAP obtained from nerves exposed to octanol 400 nM. The mean time-response curve for nerves exposed to normal saline is nearly 100% for 20 h (not shown for clarity). The bars represent ±SEM.

2.4. Sciatic nerve drug exposure protocol

The CAP of the mouse sciatic nerve immersed in normal saline solution remains constant for over 24 h (Kagiava et al., 2012) indicating that the vitality of the sciatic nerve fibers under these recording conditions is not impaired. Oxaliplatin (Tocris Bioscience) was pre-dissolved in distilled water to make the stock solution (5.0 mg/ml) and stored under light protection at −20.0 °C. Oxaliplatin from the stock was diluted in the saline contained in the perfusion (middle) chamber to make the desirable concentration, 25 μM, and single evoked CAPs were digitized and stored every 5 min throughout the 1200 min (20 h) experiment, as described above. The same procedure was followed to assess the effect of 200, 400, 600 and 2000 nM octanol, 25 and 50 μM carbenoxolone, 25 and 50 μM, 18-beta-glycyrrhetinic acid (GRA) and 100–300 μM octanoic acid (OA) (all from Sigma–Aldrich). GRA and OA were pre-dissolved in DMSO making stock solutions of 100 mM and then dissolved in saline. To assess the action of the combination of oxaliplatin and octanol we used three different conditions: a) octanol (400 nM) and oxaliplatin (25 μM) were applied simultaneously and the preparation was left for 20 h with continuous CAP monitoring as above; b) the nerve was incubated first in octanol (400 nM) for 40 min and then 25 μM oxaliplatin was added in the perfusion chamber; and c) the nerve was incubated first in 25 μM oxaliplatin for 40 min and then octanol (400 nM) was added in the perfusion chamber. Carbenoxolone, GRA, and OA were applied only simultaneously with oxaliplatin as above.

2.5. Teased fiber preparation and immunostaining

Following the *ex-vivo* electrophysiological studies, sciatic nerves exposed for either 3 or 24 h to oxaliplatin or to the combination of oxaliplatin plus octanol (above) along with control nerves (stimulated for the same time but not exposed to drugs), were fixed for 30 min in fresh 4% paraformaldehyde (PFA) (Sigma, Germany) in 0.1 M phosphate buffer (PB). Teased nerve fibers were prepared from fixed nerves, dried on SuperFrost Plus glass slides overnight at room temperature and stored at −20 °C. For immunostaining, teased fibers were permeabilized in acetone (−20 °C for 10 min) and incubated at room temperature with blocking solution (5% bovine serum albumin (BSA), 0.5% Triton-X) for 1 h, followed by primary antibodies diluted in blocking solution overnight at 4 °C. Antibodies included mouse monoclonal against Caspr (1:50; gift of Dr. Elior Peles, Weizmann Institute of Science), MBP (1:500; Abcam), SMI31 (1:5000; Abcam), PanNav (1:50; Sigma), and Na^+/K^+ ATPase-a1 subunit (1:100; Developmental Studies Hybridoma Bank, University of Iowa); rabbit antisera against Cx29 (1:300; Invitrogen), MBP (1:100; Sigma), Kv1.2 (1:200; Alomone), Caspr2 (1:100; Sigma), and Nav1.6 (1:100; Alomone), as well as goat-anti-ATPase-a3 subunit (1:100; Santa Cruz). Teased fibers were then washed in PBS and incubated with appropriate fluorescein- and rhodamine-conjugated donkey cross-affinity purified secondary antibodies (Jackson ImmunoResearch, 1:300) for 1 h at room temperature. Schwann cell nuclei were visualized with 4′,6′-diamidino-2-phenylindole (DAPI; Sigma–Aldrich). Slides were mounted with Dako Fluorescent Mounting Medium and images were photographed under a Zeiss fluorescence microscope with a digital camera using the Zeiss Axiovision software (Carl Zeiss MicroImaging, Germany). Where appropriate, we obtained images with comparable exposure times to allow better comparison between different experiments.

2.6. Electron microscopy

Following *ex-vivo* electrophysiological studies, sciatic nerves exposed to oxaliplatin or to the combination of oxaliplatin plus octanol (above) along with control nerves without pharmacological exposure, were fixed in 2.5% glutaraldehyde in 0.1 M PB overnight at 4 °C, then osmicated, dehydrated, and embedded in Araldite resin. Transverse semi-thin sections (1 μm) were obtained and stained with alkaline toluidine blue. Ultrathin sections (80–100 nm) were counterstained with lead citrate and uranyl acetate before being examined in a JEOL JEM-1010 transmission electron microscope (JEOL Ltd, Tokyo, Japan).

2.7. Neurobiotin uptake assay

Cx31.3-expressing clonal HeLa cells were generated by transfection using the human *Cx31.3* gene open reading frame (GenBank accession number AY297109) cloned into pIRESpuro3 vector as previously described (Sargiannidou et al., 2008) and maintained in selection media with puromycin (0.5 μg/ml). Expression of Cx31.3 at the cell membrane of these cells was confirmed by immunostaining and immunoblot analysis (Sargiannidou et al., 2008). For the neurobiotin uptake assay, cells permanently expressing Cx31.3 were grown to about 50–70% confluency in 4-well chamber slides, washed in PBS lacking divalent ions, pre-incubated in Optimen for 30 min, and then incubated with 2% neurobiotin (Vector Laboratories, MW: 287, 1+; diluted in HBSS) for 5–60 min, washed and fixed for 30 min in 4% PFA at 4 °C. After blocking in 5% BSA with 0.1% Triton X-100 for 30 min at RT, cells were incubated in streptavidin-Texas red (Vector Laboratories, 1:1000) at RT for 10 min, counterstained with DAPI and imaged as above. To determine the effects of oxaliplatin we performed the same experiments in the presence of oxaliplatin alone (25 and 50 μM) or oxaliplatin in combination with octanol (200 nM–2000 nM) diluted in Optimem for 30 min before and during incubation with neurobiotin.

For quantitative analysis of neurobiotin uptake with or without addition of oxaliplatin and octanol in Cx31.3 expressing cells, the mean red channel pixel intensity was measured in images captured with constant time exposures using the *ImageJ* software (NIH image). At least 2000 cells in each condition were compared. Statistical significance was examined using the Student's t-test. All experiments were performed in triplicates.

2.8. Neurobiotin scrape loading assay

Cx32 expressing clonal HeLa cells were plated on 6-well plates to reach ~90–100% confluency on the day of the scrape loading. For neurobiotin scrape

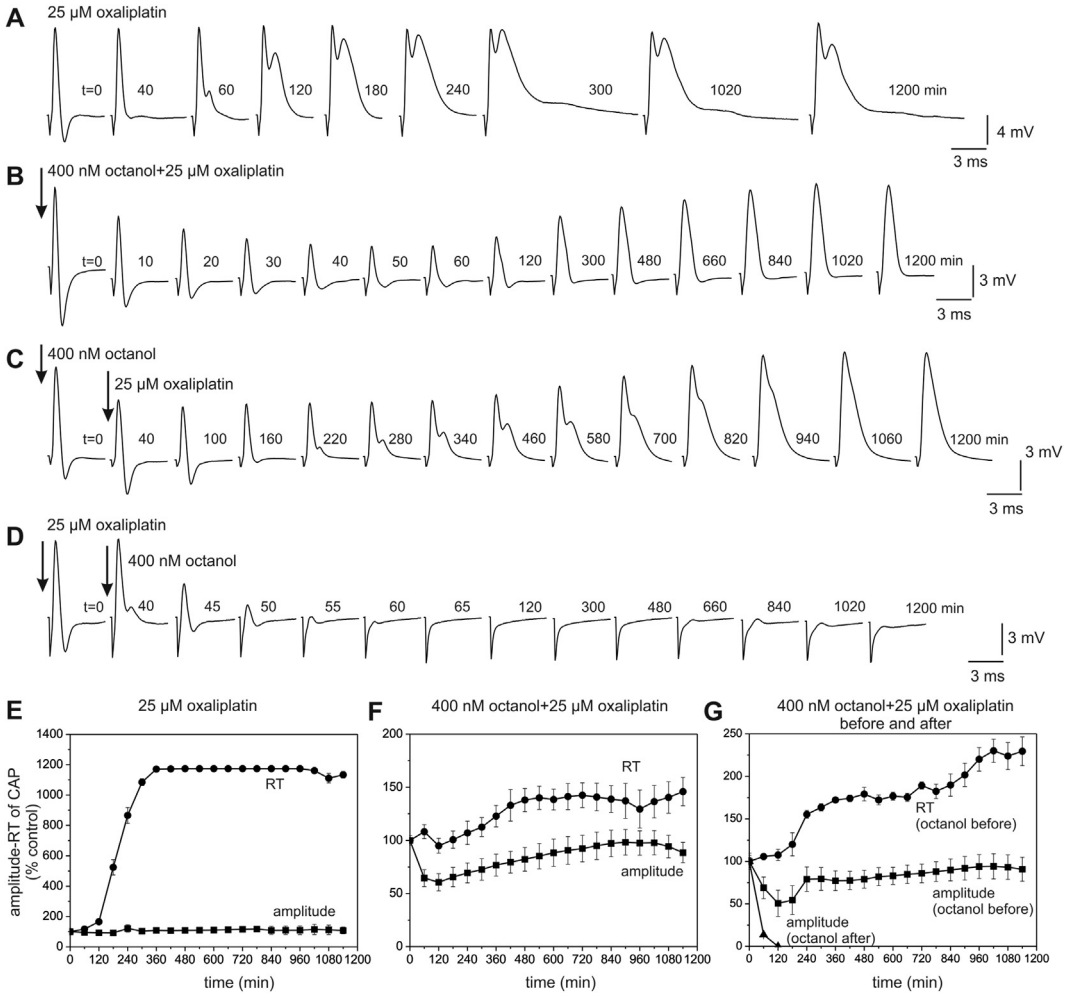

Fig. 2. The neurotoxic effect of oxaliplatin and neuroprotective effect of octanol on the isolated mouse sciatic nerve: Representative recordings of the evoked CAP (time point of each CAP recording is indicated by t) from nerves (A) incubated in 25 μM oxaliplatin; (B) incubated simultaneously in 400 nM octanol and 25 μM oxaliplatin; (C) incubated first in 400 nM octanol (first arrow) and then 25 μM oxaliplatin was added (second arrow) in the perfusion chamber; (D) incubated in first in 25 μM oxaliplatin (first arrow) and then 400 nM octanol was added (second arrow) in the perfusion chamber. (E) The mean time-response curves represent the percentage change in amplitude and RT (marked on the curves) of the evoked CAP incubated in 25 μM oxaliplatin, as a fraction of incubation time (n = 6). The amplitude of the evoked CAP at time 0, before the application of oxaliplatin, was considered to be 100%. (F) as in (E) but the nerves were incubated in a mixture of 400 nM octanol and 25 μM oxaliplatin (n = 5). (G) as in (E), but the nerves were either first incubated in 400 nM octanol for one hour and then 25 μM oxaliplatin was added (n = 4; octanol before), or oxaliplatin was applied first and then octanol added (n = 3; octanol after, only the plot of the initial CAP amplitude is shown). The bars represent ±SEM.

loading, cells were rinsed 3 times in HBSS without calcium or magnesium and 1% neurobiotin was added alone, or in combination with either octanol 400 nM, oxaliplatin 25 μM, or with both octanol and oxaliplatin. A scalpel blade was used to cut a grid for scraping the cells, and then cells were incubated in neurobiotin for 15 or 30 min, washed 3 times in HBSS, fixed with cold 4% paraformaldehyde (PFA) for 10 min, washed 3 times in PBS, blocked in 5% BSA with 0.1% Triton X-100 for 30 min at RT, incubated in streptavidin-rhodamine (Vector Laboratories, diluted 1:300) at RT for 1 h, washed 3 times in PBS, 3 times in H_2O, incubated with DAPI for 5 min at RT, washed, dried, and pictures were taken as above. For quantification of gap junctional connectivity, the number of fluorescent cells in a rectangle on one side of the scrape line but excluding cells that were in the scrape line were counted and the mean ± SEM were calculated for each condition and compared with the Student's t-test.

3. Results

3.1. The effects of octanol on the sciatic nerve CAP

The evoked CAPs generated by 1 Hz supramaximal stimulation of the mouse sciatic nerve representing the summation of action potentials of all activated sciatic nerve fibers (100% of myelinated nerve fibers) showed constant amplitudes over the 20–24 h recording period (Fig. 1A), followed by a gradual decrease due to nerve fiber inactivation, as in our previous studies (Kagiava et al., 2012). Thus, the vitality of the sciatic nerve fibers is not affected by the recording conditions in the first 1200 min (20 h) of the experiment. Although nerve vitality lasts longer than 1200 min (Fig. 1A), the incubation period with the compounds under investigation lasted for maximum of 1200 min. This was the period where the probability to record CAPs of a constant amplitude and duration was 100%. Beyond that time the CAP became unstable in some experiments, therefore we assessed CAPs recorded only up to 1200 min exposure times to ensure reliability of the results.

In order to investigate the role of myelin GJs and hemichannels in the generation of action potentials of the nerve fibers and in extend of the CAP, we first examined the effects of the GJ blocker octanol. Since previous studies suggested that octanol may inhibit VGNaCs expressed in *Xenopus* oocytes with an IC_{50} of 72.1 ± 4.5 μM within a range of 0.003 (min) – 3 mM (max) (Horishita and Harris, 2008), we used octanol concentrations of 200, 400, 600 and 2000 nM, far below the minimum concentration required to inhibit VGNaCs. When the nerve was exposed to 200 nM octanol there was

a minor, 10–20% decrease in the evoked CAP at the beginning of the 1200 min exposure (representative recordings in Fig. 1B and mean time–response curve from n = 4 different experiments in Fig. 1E). At a concentration of 400 nM octanol caused a nearly 50% decrease of the initial value of the CAP almost immediately after application (Fig. 1C, records t = 10–60 min) followed by a gradual recovery (records t = 300–1200 min). The mean time-response curve (400 nM in Fig. 1E) showed a CAP decrease to 46.5 ± 10.69% of its original value (n = 6) within 1 h, while by 6 h of exposure the CAP recovered to 65.1 ± 10.97% and remained at this level despite continuous exposure to octanol. Application of 600 nM octanol caused a sharp decrease of the CAP amplitude to 42.3 ± 10.28% within 1 h, gradually complete elimination of the CAP within 6–7 h, and no recovery even after 20 h (600 nM in Fig. 1D–E; n = 4). Finally, application of 2000 nM octanol eliminated completely the CAP amplitude within 1 h, without any recovery (2000 nM in Fig. 1E; n = 4). Thus, octanol caused a concentration-dependent reversible decrease in CAP amplitude at 200 and 400 nM, whereas a permanent elimination with loss of active nerve fibers occurred at 600–2000 nM, called here the "octanol-effect". In contrast to the inhibitory effect on CAP amplitude, exposure to octanol had no effect on the duration of the CAP. For example, at 400 nM the duration of the CAP remained constant (duration curve in Fig. 1E, open triangles).

3.2. Oxaliplatin prolongs the repolarization time (RT) of the sciatic nerve CAP

Incubation of mouse sciatic nerve with oxaliplatin caused a drastic, time-dependent, increase in the repolarizing time (RT) of the CAP (Fig. 2A), similar to our previous findings in the rat sciatic nerve (Kagiava et al., 2008, 2013). The effect started with a gradual decrease of the negative part of the CAP repolarising phase (Fig. 2A, records t = 0 to t = 40 min). The increase in RT, measured from the peak of the CAP to the point where the repolarising phase meets the baseline, started from 2.39 ± 0.08 ms under control conditions and reached 26.2 ± 0.16 ms after 300 min of exposure ($P < 0.01$; n = 8 experiments) remaining at this level for 1200 min. Furthermore, in all eight experiments a second peak occurred on the main CAP almost at the beginning of the exposure (Fig. 2A, t = 60 min) and persisted to the end of continuous recordings (t = 1200 min). The mean time-response curve with a per-minute sampling rate showed that the RT increased up to 1173.8 ± 0.92% (n = 8) of the control values and remained at this level throughout the 1200 min exposure to oxaliplatin (Fig. 2E, RT). This abrupt increase in the RT is called here the oxaliplatin-effect. This broadening of the CAP recorded extracellularly in the presence of oxaliplatin results from broadening in the action potential of individual sciatic nerve fibers, as shown by previous intra-axonal recordings (Kagiava et al., 2013). In contrast to RT, we found no significant change in the CAP amplitude at the initial (t = 60 min) and at the final stages (t = 1200 min) of the recording under 25 μM oxaliplatin exposure ($P > 0.05$, n = 8) (Fig. 2E). Importantly, the duration of the CAP depolarizing phase reflected by the rise time of the CAP, during which the VGNaCs are activated, remained unchanged.

3.3. Co-application of octanol and oxaliplatin abolishes the effects of oxaliplatin

In order to test the possible protective role of the GJ inhibitor octanol against OIN we exposed the sciatic nerve to 25 μM oxaliplatin and 400 nM octanol, both applied in the perfusion chamber simultaneously. The 400 nM octanol concentration was chosen because it had an intermediate inhibitory effect when applied alone (Fig. 1C), without a drastic neurotoxic effect as seen with higher concentrations (600 nM, Fig. 1D). This co-application had an effect on both amplitude and RT of CAP. The CAP amplitude decreased within the first hour of exposure with gradual, almost full recovery after 3–15 h (Fig. 2B), resembling the octanol-effect at 400 nM (Fig. 1C and E). Interestingly, there was a much smaller increase in the RT of the CAP, in contrast to the marked increase observed when 25 μM oxaliplatin was applied alone (Fig. 2A). During co-application, the oxaliplatin-effect started with a loss of the negative phase of CAP repolarization in the first hour (Fig. 2B, records t = 0 to t = 60 min), but at this point the oxaliplatin-effect stopped, and there was no further increase in the RT, which remained stable ranging from 2.33 to 3.92 ms (Fig. 2B, record t = 120 to t = 1200 min), indicating that octanol abolishes the effect of oxaliplatin. The RT mean time-response curve (Fig. 2F), obtained from n = 5 experiments indicates that the octanol-effect dominated over the oxaliplatin-effect. During co-application the effect of octanol developed as a fast decrease of the CAP amplitude to 60.6 ± 8.08% of the control values within 1 h, followed by a relatively slow recovery within 2–12 h. On the other hand, the oxaliplatin-effect, the broadening of the CAP, was almost eliminated and restricted drastically to an increase in the RT of the CAP up to 146.0 ± 13.29% of the initial value (Fig. 2F), in contrast to the >1173.75% increase in the presence of oxaliplatin alone ($P < 0.05$) (Fig. 2E). This is a clear indication of neuroprotection of octanol against oxaliplatin-induced neurotoxicity which reaches 88.6%. Interestingly, oxaliplatin also provided mild "neuroprotection" against the octanol-effect. While the maximum recovery of the CAP amplitude when a nerve was exposed to 400 nM octanol only was at the level of 64.0 ± 7.0% at 1200 min (Fig. 1E), co-administration of octanol (400 nM) and oxaliplatin (25 μM) resulted in higher recovery levels up to 98.2 ± 12.04% ($P < 0.01$) (Fig. 2F).

Addition of octanol 40 min prior to oxaliplatin incubation resulted in weaker protection, while the octanol-effect, the decrease and recovery of the CAP, persisted (Fig. 2C). The mean time-response curve under these conditions (n = 4 experiments) showed an increase of the RT of CAP by 189.2 ± 4.28% in the first 12 h of exposure and then further to 230.1 ± 13.65% (Fig. 2G), significantly higher compared to the corresponding experiment of co-application ($P < 0.05$). Nevertheless, even with pre-application octanol offered an 81.4% protection against OIN while the octanol-effect (decrease and recovery of the CAP amplitude) followed the same pattern as in the previous experiments (Fig. 2G). In contrast, when oxaliplatin was added first followed after 40 min by octanol, the CAP was eliminated completely within less than 60 min, without any recovery after 1200 min, indicating that this particular sequence was extremely toxic for the sciatic nerve fibers (Fig. 2D, G; n = 4). Thus, only when octanol (400 nM) was applied simultaneously or prior to oxaliplatin (25 μM) was there a significant protection against the oxaliplatin-effect on sciatic nerve fiber function.

3.4. Concentration-dependent neuroprotection by octanol against the oxaliplatin-effect

To investigate whether the neuroprotection was concentration-dependent 200 and 600 nM octanol were also tested against the oxaliplatin-effect. During co-application of 200 nM octanol plus 25 μM oxaliplatin there was a weaker neuroprotection with increasing RT of the CAP followed by weak development of a second peak of the waveform (Fig. 3A, record t = 120–1200 min), which never occurred in the previous treatment (400 nM octanol + 25 μM oxaliplatin). The mean time-response curves showed that the increase in the RT reached a maximum of 172.3 ± 10.07%, significantly higher than with the 400 nM + 25 μM combination ($P < 0.05$) (Fig. 3C). Nevertheless, even at this low concentration (200 nM)

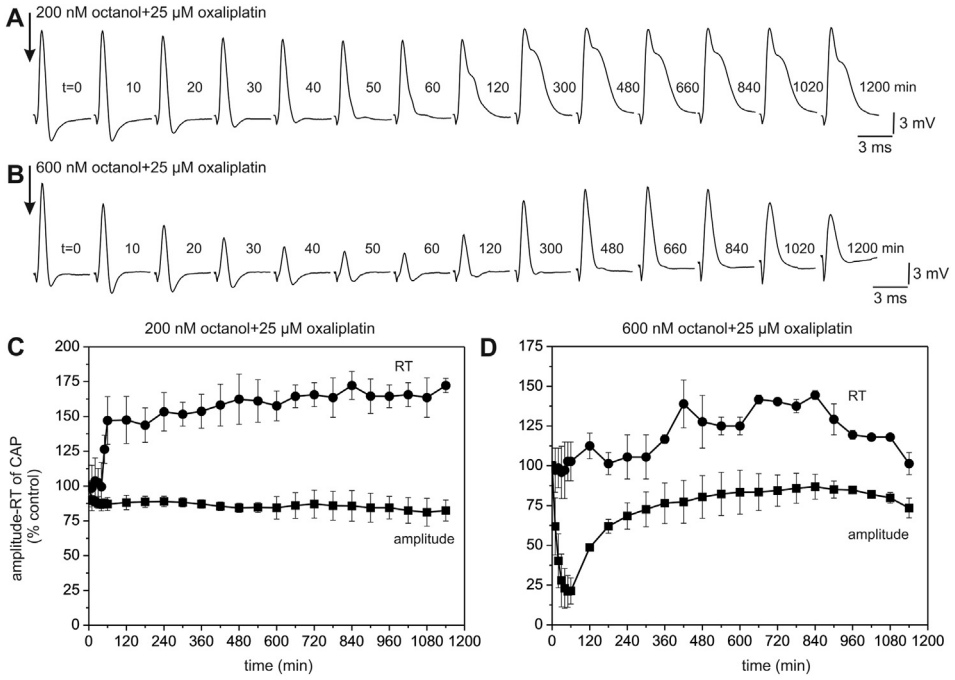

Fig. 3. Concentration-dependent neuroprotection of octanol against oxaliplatin-induced neurotoxicity in the mouse sciatic nerve: (A) Recordings of the evoked CAP from a nerve immersed simultaneously in 200 nM octanol and 25 μM oxaliplatin. The time of exposure of the nerve to oxaliplatin for each CAP is indicated (t in min). (B) as in (A) but the nerve was incubated in the mixture of 600 nM octanol and 25 μM oxaliplatin. (C) Mean time-response curves (RT and amplitude as indicated) obtained from 200 nM octanol/25 μM oxaliplatin co-exposure (n = 4) as in A. (D) Mean time-response curves obtained from 600 nM octanol/25 μM oxaliplatin co-exposure as in B (n = 3). The amplitude and RT of the evoked CAP at time 0, before the application of the mixture of octanol and oxaliplatin, was considered to be 100%. The bars represent ± SEM.

octanol offers a significant (85.3%) protection against OIN, very close to the one at 400 nM (88.6%), while the octanol-effect was milder with an amplitude decrease of 16% and a relatively slow recovery (Fig. 3C).

The neurotoxic effect of 600 nM octanol, the elimination of the CAP (Fig. 1E), was abolished in the presence of oxaliplatin. This mixture minimized the amplitude of the CAP to 21.0 ± 10.03% within 1 h (n = 3) (Fig. 3B and D), as 600 nM octanol did when applied alone (Fig. 1E), but within 3–5 h instead of eliminating the amplitude of the CAP, there was a recovery up to 86.8 ± 7.80% (Fig. 3B and D). Furthermore, during this unexpected inhibition-recovery of the CAP by 600 nM octanol, octanol protected against the oxaliplatin-effect, resulting in an increase of RT up to 144.5 ± 2.77% (n = 3), far smaller compared to changes caused by oxaliplatin alone ($P < 0.05$) (compare Fig. 3B, D and Fig. 2A, E). Thus, even at a higher concentration of 600 nM octanol combined with oxaliplatin (25 μM) resulted in a significant (87.7%) neuroprotection against the oxaliplatin-effect, offering overall a wider therapeutic window with a concentration-dependent effect on nerve fiber dysfunction.

3.5. Oxaliplatin-effect and neuroprotection by octanol are weaker in Cx32 knockout nerves

Since octanol is considered to be a non-specific GJ blocker, there are two known potential targets to mediate its protective effects against oxaliplatin in myelinated nerve fibers of the mouse sciatic nerve: Cx32, which forms GJs through the layers of non-compact myelin at paranodes and Schmidt–Lantermann incisures (Scherer et al., 1995), and Cx29, which forms GJ hemichannels rather than full GJs at the innermost myelin membrane apposing axonal juxtaparanodes and juxtaincisures (Altevogt et al., 2002). In order to distinguish the relevant connexin mediating the protective effects of octanol, we performed the same experiments as above in *ex vivo* sciatic nerves of Cx32 KO as well as Cx29 KO mice. In both Cx32 KO and Cx29 KO nerves examined under control conditions (n = 3 nerves per genotype) using the same recording bath, the CAP generated by 1 Hz stimulation remained constant in amplitude and duration for 1200 min. The recordings were identical to those obtained from WT nerves ($P > 0.05$), indicating that the vitality and physiological properties of sciatic nerves from either connexin KO animals were not affected by the specific stimulating and recording conditions (*data not shown*).

Application of 25 μM oxaliplatin on Cx32 KO nerves resulted in a marked increase in the RT of the CAP (Fig. 4A), while the distinct second peak observed in the recordings from the WT sciatic nerves (Fig. 2A) was absent in all Cx32 KO nerves examined changing significantly the shape of the CAP waveform. The mean time-response curve from n = 9 Cx32 KO nerves (Fig. 4D) showed that the RT broadening reached a maximum of 683.9 ± 36.5% (from 3.1 ± 0.25 to 22.7 ± 1.31 ms, $P < 0.01$) within 360 min, but then decreased significantly reaching a value of 430.3 ± 62.08% ($P < 0.05$) near the end of the experiment (960–1080 min); these changes were significantly smaller compared to WT nerves, where RT was prolonged by 1170.8 ± 1.86% at 360 min ($P < 0.05$) and remained constant throughout the 1200 min experiment (Fig. 2E). Shorter RT in the Cx32 KO CAP could be due to the absence of the second peak. As in WT nerves the CAP amplitude was not significantly affected during treatment in Cx32 KO nerves (Fig. 4D). Thus, the oxaliplatin-effect develops only partially in Cx32 KO nerves, showing some similarities, but also important differences compared to nerves from WT animals.

In order to examine whether octanol remains neuroprotective against oxaliplatin also in Cx32 KO nerves, we first clarified the effects of octanol alone. Application of 400 nM octanol caused the same pattern of the inhibitory-recovery effect on CAP amplitude as in WT nerves (Fig. 4B). However, the RT mean time-response curve from Cx32 KO nerves showed a 30% ($P < 0.05$; n = 4) increase at the

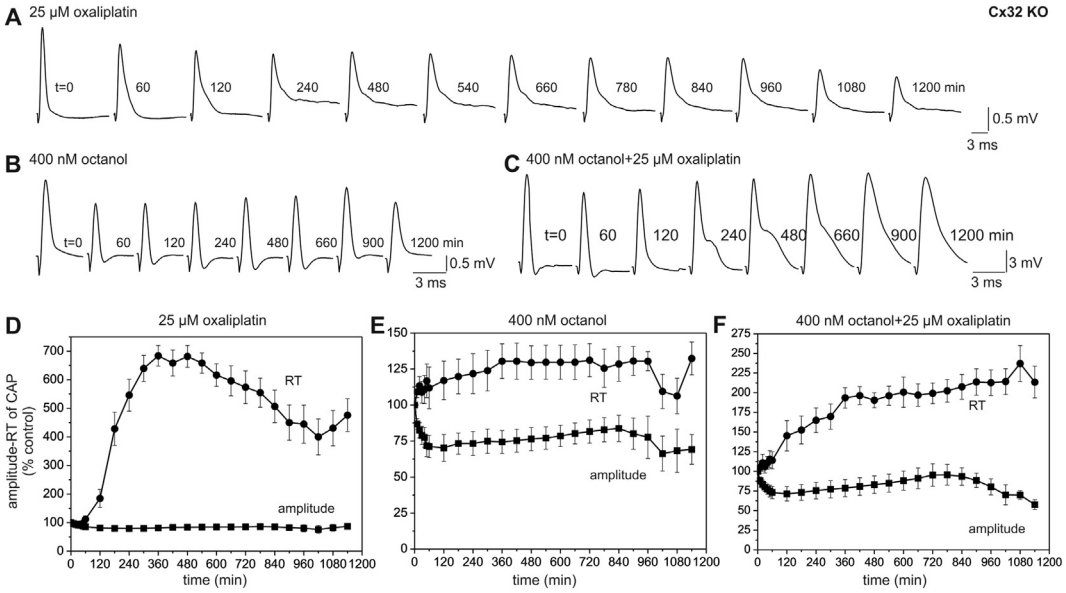

Fig. 4. The effects of octanol, oxaliplatin and their mixture on the evoked CAP recorded from the isolated sciatic nerve of the Cx32 knockout (KO) mouse. Recordings of the CAP from Cx32 KO nerves incubated in 25 μM oxaliplatin (A), in 400 nM octanol (B), or in a mixture of 400 nM octanol and 25 μM oxaliplatin (C). The time of recording of each CAP is indicated (t in min). D–F: Diagrams showing the mean time-response curves of the CAP amplitude and RT recorded from Cx32 KO nerves during the exposure to 25 μM oxaliplatin (n = 9) (D), to 400 nM of octanol (n = 4) (E), or to the mixture of 400 nM of octanol and 25 μM oxaliplatin (n = 6) (F). The CAP amplitude and RT at time 0 before drug exposure was considered to be 100%. The bars represent ± SEM.

beginning of the exposure which remained at this level throughout the experiment (Fig. 4E), in contrast to WT nerves which showed almost constant RT (near 100%) when exposed to 400 nM of octanol. Thus, the octanol-effect occurred also in Cx32 KO nerves but in slightly different pattern compared to WT nerves.

Finally, co-application of 25 μM oxaliplatin plus 400 nM octanol in Cx32 KO nerves protected against the broadening of the RT, the oxaliplatin-effect (Fig. 4C). The mean time-response curve (Fig. 4F, n = 6) clearly indicated that the RT reached 193.5 ± 12.93% of the initial value ($P < 0.01$ comparison to oxaliplatin alone) after treatment for 360 min and then remained at this level for most of the duration of the experiment, before showing a further increase to 237.2 ± 23.0% near the end of the experiment (t = 1080 min). However, the octanol neuroprotection against oxaliplatin-effect was significantly weaker in Cx32 KO nerves (71.7%) compared to WT (88.6%) in which RT increased only to 146.0 ± 13.29% ($P < 0.05$). Besides the neuroprotection of octanol against oxaliplatin in Cx32 KO nerves, there was also an obvious protective action of oxaliplatin against the octanol-effect, as also observed in WT nerves. In Cx32 KO nerves treated with 400 nM octanol the amplitude of the CAP recovered only up to 83.7 ± 9.12% after 840 min (Fig. 4E), while in nerves treated with octanol combined with oxaliplatin the maximum recovery tended to be larger, 93.5 ± 11.06% ($P > 0.05$), and appeared also at the same time as in the previous experiments, after 840 min (Fig. 4F). In conclusion, the results in Cx32 KO nerves indicate that the effects of oxaliplatin as well as the protective action of octanol occurred but were significantly weaker compared to WT, implicating Cx32 GJ channels, at least in part, in OIN.

3.6. Oxaliplatin-effect and neuroprotection largely persist in Cx29 knockout nerves

Application of 25 μM oxaliplatin on Cx29 KO nerves resulted in a marked increase in the RT of CAP (Fig. 5A). Also, in all Cx29 KO nerves examined, the distinct second peak appeared as it was observed in the recordings from the WT nerves (compare Figs. 2A and 5A). The RT mean time-response curve from n = 3 Cx29 KO nerves (Fig. 5C) showed that the RT was prolonged to a maximum of 1035.0 ± 44.74% in 400–600 min and then declined to 441.3 ± 62.10% near the end of the experiment (1200 min). This unusually fast increase and unstable reduction of RT, indicated by large variations after 900 min (Fig. 5C) could be due to the gradual decrease of CAP after 600 min of exposure to oxaliplatin (Fig. 5A and C). Such drastic changes in these two parameters were not observed in either WT or Cx32 nerves. Thus, the oxaliplatin-effect develops also in Cx29 KO nerves showing important similarities and minor differences compared to WT nerves.

Exposure of Cx29 KO nerves to the combination of oxaliplatin (25 μM) and octanol (400 nM) showed a significant (87.1%) neuroprotection, with a maximum RT increase of only 132.8 ± 4.92% (Fig. 5D; n = 3). Thus, the degree of neuroprotection offered by octanol against the oxaliplatin effect in Cx29 KO nerves was not different from WT nerves (88.6%; $P > 0.05$), whereas in was clearly stronger than in Cx32 KO nerves (71.7%; $P < 0.05$). Taken together, the findings from Cx32 KO and Cx29 KO nerves suggest that oxaliplatin affects the function of both Cx32 GJ channels and Cx29 hemichannels, but the effect on Cx32 appears to be more prominent compared to Cx29.

3.7. Effects of other gap junction blockers against OIN

Based on the results of octanol we examined whether another three GJ blockers, carbenoxolone, GRA and OA, could have a neuroprotective effect against OIN. We first estimated the concentration with the minimum neurotoxicity on the sciatic nerve. Carbenoxolone at 50 μM was found to be extremely neurotoxic eliminating the CAP in 120–300 min (n = 4), while at 10 and 25 μM (n = 4 each) carbenoxolone had a milder effect causing a 20% decrease at the beginning of exposure and then a recovery within 1200 min (Fig. 6A). However, at this non-toxic concentration of 25 μM, carbenoxolone failed to provide neuroprotection against the oxaliplatin-effect when tested in simultaneous administration with 25 μM oxaliplatin (n = 4) (Fig. 6D), since RT increased up to 1107.1 ± 36.79%.

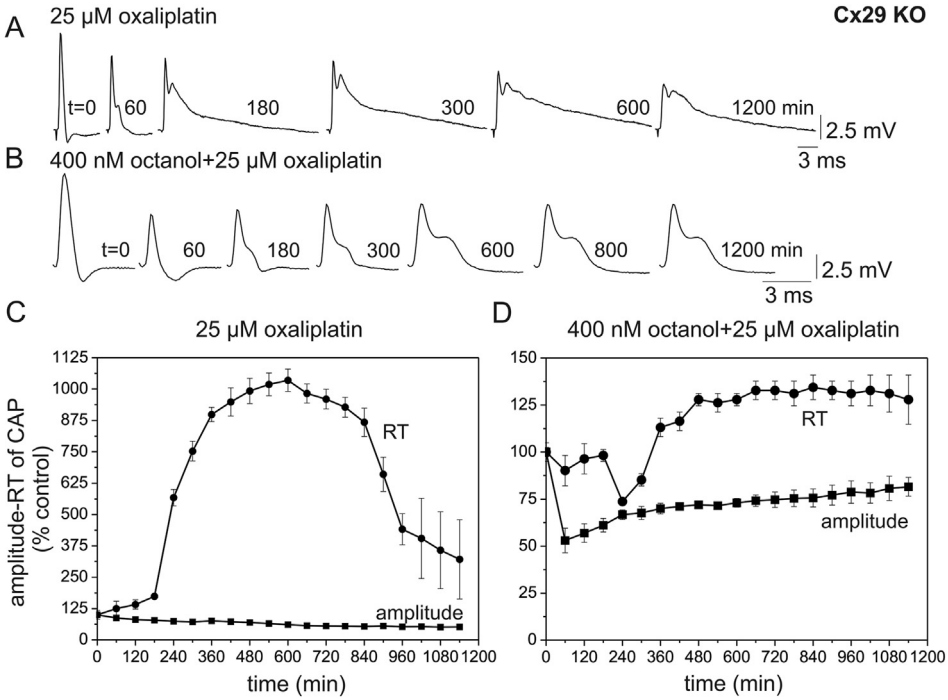

Fig. 5. The effects of octanol, oxaliplatin and their mixture on the evoked CAP recorded from the isolated sciatic nerve of the Cx29 KO mouse. Recordings of the CAP from Cx29 KO nerves incubated in 25 μM oxaliplatin (A) and in a mixture of 400 nM octanol and 25 μM oxaliplatin (B). The time of recording of each CAP is indicated (t in min). C–D: Diagrams showing the mean time-response curves of the CAP amplitude and RT recorded from Cx32 KO nerves during the exposure to 25 μM oxaliplatin (n = 3) (C), or during exposure to the mixture of 400 nM of octanol and 25 μM oxaliplatin (n = 3) (D). The CAP amplitude and RT at time 0 before drug exposure was considered to be 100%. The bars represent ± SEM.

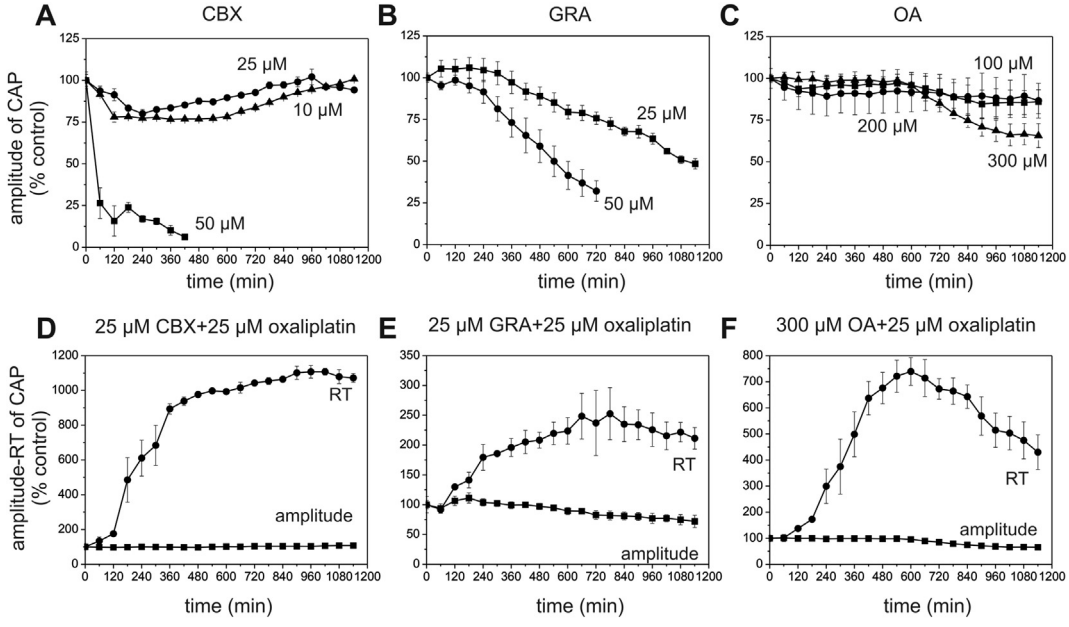

Fig. 6. A–C: Concentration-dependent effects of carbenoxolone (CBX), 18-beta-glycyrrhetinic acid (GRA) and octanoic acid (OA) on the mouse sciatic nerve. CBX is toxic at 50 μM rapidly reducing CAP amplitude, while it is only minimally toxic up to 25 μM (A). GRA also shows toxicity at 50 μM and to a lesser degree at 25 μM, that develops more gradually (B). OA starts having mild toxic effects at 300 μM (C). When co-administered with 25 μM oxaliplatin, carbenoxolone fails to show any protective effect at a non-toxic concentration (D), while GRA at 25 μM shows significant neuroprotection ameliorating RT prolongation by 78.8% (E), and OA at 300 μM shows a modest protection of 37.6% (F).

Using the same protocol, 50 μM GRA were found to be neurotoxic, decreasing the CAP amplitude to 25% of the control within 720 min (Fig. 6B), while 25 μM of GRA proved to be less toxic maintaining the CAP amplitude near 50% of its original value (Fig. 6 B). Co-application of 25 μM GRA and 25 μM of oxaliplatin showed a significant neuroprotection since the RT increased only up to 248.5 ± 38.39% (Fig. 6E), instead of 1173.8 ± 0.92% when oxaliplatin was applied alone (78.8% neuroprotection, $P < 0.01$). Furthermore, as already shown with octanol (above), we observed a protection of oxaliplatin against the inhibitory effect of GRA on the CAP

amplitude. 25 μM GRA alone decreased the CAP to 50% (Fig. 6B), while in the presence of oxaliplatin only to 75% of baseline ($P < 0.05$). Thus, GRA provides a similar neuroprotection against OIN as seen with octanol, although with a smaller therapeutic window.

Finally, three concentrations, 100, 200 and 300 μM of OA were tested ($n = 3$ each). The first two had only a minor effect on the vitality of nerve fibers, since the CAP remained at the same level throughout the exposure (1200 min) (Fig. 6C), while the concentration of 300 μM caused a decrease of the CAP to 65.6 ± 7.17% (Fig. 6C). Co-application of the high concentration of 300 μM with 25 μM oxaliplatin had only a mild protective effect (37.6% protection), since the increase of RT reached 731.6 ± 53.24%, compared to 1173.8 ± 0.92% when oxaliplatin was applied alone ($P < 0.05$).

3.8. Morphological changes caused by the prolonged exposure to oxaliplatin

In order to examine whether there is a morphological correlate to the functional changes caused by oxaliplatin in peripheral nerve fibers described above, we also immunostained teased fibers from sciatic nerves following the 20 h *ex vivo* study. Most fibers were well preserved and were double stained with myelin and axonal markers, as well as markers of axonal domains including Nav1.6/PanNav at nodes, Kv1.1 or Caspr2 at juxtapanodes and Caspr at paranodes, in combination with Cx29. Fibers from sciatic nerves exposed to oxaliplatin for 20 h frequently showed a characteristic enlargement of juxtaparanodal axonal areas, which appeared to cause a thinning of the surrounding myelin and retraction away from paranodal areas (Fig. 7B, E). The characteristic myelin loops surrounding the paranodes that are seen in control fibers were thinner or not visible. However, the localization of Cx29, Kv1.1, Caspr2, Caspr and Nav was not disturbed, indicating that axonal domains were preserved (Fig. 7D–L). Na^+/K^+ ATPase a1 subunit along the axon and a3 subunit in non-compact myelin areas were also preserved (Fig. 7M–O). Juxtaparanodal swelling was not seen in fibers treated with the combination of oxaliplatin and octanol or in untreated fibers that were also stimulated for 20 h with same frequency (Fig. 7A, C). These morphological changes were not found in nerves examined after a short exposure to oxaliplatin for 3 h (*data no shown*), despite significant broadening in the repolarizing phase of the evoked CAP at this time point (Fig. 2A), suggesting that functional changes are initially not accompanied by morphological changes, and that juxtaparanodal swelling occurs only with longer oxaliplatin exposure.

To further clarify the nature of the morphological changes observed by immunostaining, we also examined semithin and ultrathin sections of *ex vivo* stimulated nerves exposed to each condition and control nerves. In semithin sections of nerves exposed to oxaliplatin, we observed a widening of axonal diameter at

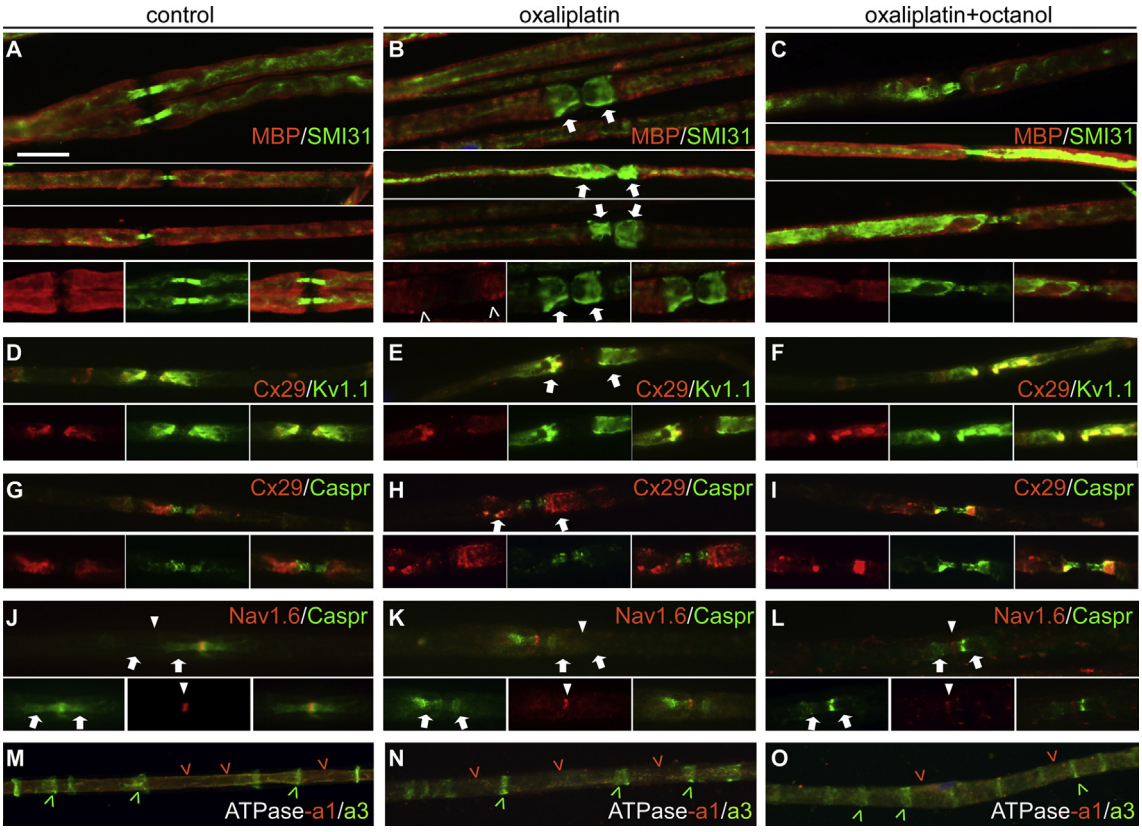

Fig. 7. Juxtaparanodal abnormalities in myelinated fibers after prolonged oxaliplatin exposure *ex vivo*. Images of sciatic nerve teased fibers obtained from control sciatic nerves exposed to normal saline (A, D, G, J, M) and nerves exposed to 25 μM oxaliplatin alone (B, E, H, K, N) or combined with 400 nM octanol (C, F, I, L, O). All nerves were placed in the recording bath under continuous 1 Hz stimulation for over 24 h. Both merged images and insets with separate channels underneath are shown. Fibers were immunostained with axonal marker SMI31 (green) and myelin basic protein (red) in A–C, with Cx29 (red) combined with juxtaparanodal Kv1.1 (D–F) or with paranodal Caspr (G-I) (green), with nodal Nav1.6 (red) combined with Caspr (green) (J–L), as well as for Na^+/K^+ ATPase a1 subunit along the axon (red open arrowheads) and α3 subunit at the incisures (green open arrowheads) (M–O), as indicated. In control fibers nodes are surrounded by paranodal myelin forming loops around the axon, whereas in fibers exposed to oxaliplatin there is a widening of SMI31 immunoreactivity at paranodal and juxtaparanodal areas (arrows) and the surrounding myelin sheath is thinner and appears retracted away from nodes. This abnormality is not seen in fibers treated with oxaliplatin plus octanol. Double labeling with Cx29 and Kv1.1 or Caspr and Nav1.6 with Caspr shows the widening of juxtaparanodes in fibers exposed to oxaliplatin (E), although the organization of axonal domains and localization of Nav1.6 and Kv1.1 channels and ATPase subunits is not altered. Scale bar: 10 μm.

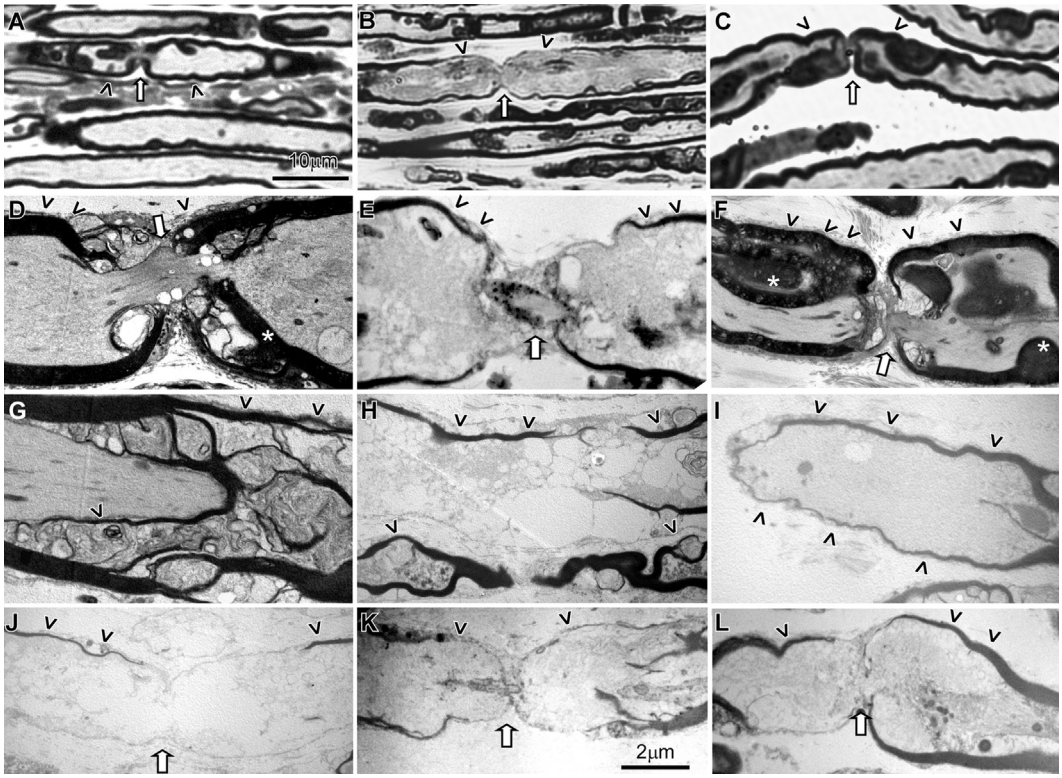

Fig. 8. Ultrastructural changes in sciatic nerve myelinated fibers after prolonged exposure to oxaliplatin and prevention by octanol. A–C: Images of longitudinal semithin sections from *ex vivo* stimulated sciatic nerves treated with oxaliplatin alone (B) or in combination with octanol (C) or control treated with saline (A). Nodal areas are indicated (arrows), demonstrating in the control nerve the normal architecture of the perinodal areas (open arrowheads), with myelin sheath forming paranodal loops. In contrast, the oxaliplatin treated nerve shows widening of the paranodal and juxtaparanodal area of the axon, causing an obliteration of the paranodal myelin loops, thinning and retraction of the myelin away from the node. Images of ultrathin sections (D–L) confirm the widening of paranodal areas showing a homogeneous axonal area with reduced density consistent with edema and lack of any inclusions in oxaliplatin treated fibers (E, H–L), while nodal structures are preserved (E, K). This axonal swelling is associated with thinning and flattening of perinodal myelin, obliteration of septate junctions and retraction of myelin from paranodal areas (arrowheads). Normal axonal domains, septate junctions, paranodal myelin loops (stars) and normal juxtaparanodal myelin thickness can be seen in the control fibers (D) and in oxaliplatin plus octanol treated fibers (F). Similar axonal swelling and thinning of the myelin sheath in oxaliplatin treated nerves can be seen in axonal areas surrounded by Schmidt–Lantermann incisures (H), as opposed to the normal appearance of juxta-incisures in control nerves (G). Scale bars: in A–C 10 μm; in D–L: 2 μm.

juxtaparanodes, and obliteration of the surrounding myelin sheath (Fig. 8B). These changes were not observed in control nerves or in nerves treated with the combination of oxaliplatin and octanol (Fig. 8A, C). Further examination of these axonal changes by electron microscopy showed that swollen perinodal areas were edematous, and did not contain any dense or aggregated material. In addition, the axonal cytoskeletal elements such as microtubules, neurofilaments and associated mitochondria, which are normally dense in perinodal areas, were rarefied. The septate axon-glial paranodal junctions were obliterated and the surrounding myelin sheath appeared retracted and thinner over the edematous paranodal and juxtaparanodal axonal areas. Nodal structures were clearly preserved in most swollen axons (Fig. 8E, I–L). Similar edematous axonal swellings were observed in axonal areas surrounded by Schmidt–Lantermann incisures (Fig. 8H). Thus, prolonged (20 h) exposure to oxaliplatin causes profound morphological changes in axons, in addition to the functional changes that occur within the 3 h of oxaliplatin exposure and are initially not accompanied by any morphological changes.

3.9. Oxaliplatin causes increased opening of Cx31.3 hemichannels and Cx32 GJ channels in vitro

Our electrophysiological experiments indicated that oxaliplatin effects on the peripheral nerve may be mediated in part through Cx29 hemichannels localized at the inner myelin membrane in close apposition to axonal VGKCs. To further investigate this possibility, we studied the effects of oxaliplatin on clonal HeLa cells expressing the human ortholog of Cx29, Cx31.3, which have been shown to form functional hemichannels on the cell surface (Sargiannidou et al., 2008). Cx31.3 hemichannel function was assessed by the neurobiotin uptake assay. Cx31.3 expressing cells were incubated with or without the addition of oxaliplatin (25 and 50 μM concentrations). Neurobiotin uptake increased over time reaching a plateau after one hour in unexposed Cx31.3 cells (Fig. 9D), while in the presence of oxaliplatin, neurobiotin uptake was accelerated, reaching a plateau already after 20 min of exposure, and was significantly increased at all time points examined ($P < 0.05$) (Fig. 9E) indicating forced opening of Cx31.3 hemichannels. These results were confirmed by quantitative analysis in at least 3 independent experiments with counts of neurobiotin signal intensity in at least 2000 cells per time point (Fig. 9G). This effect of oxaliplatin on neurobiotin uptake was blocked by octanol (200–1000 nM) in a dose-depended manner ($P < 0.05$) (examples in Fig. 9F and quantification from 3 independent experiments in H), confirming that it is mediated through opening of Cx31.3 hemichannels. Thus, oxaliplatin appears to open GJ hemichannels, an effect that can be blocked by octanol. Furthermore, oxaliplatin has similar effects on Cx31.3, the human ortholog of rodent Cx29, assessed in clonal cells, supporting the relevance of this effect for OIN in humans.

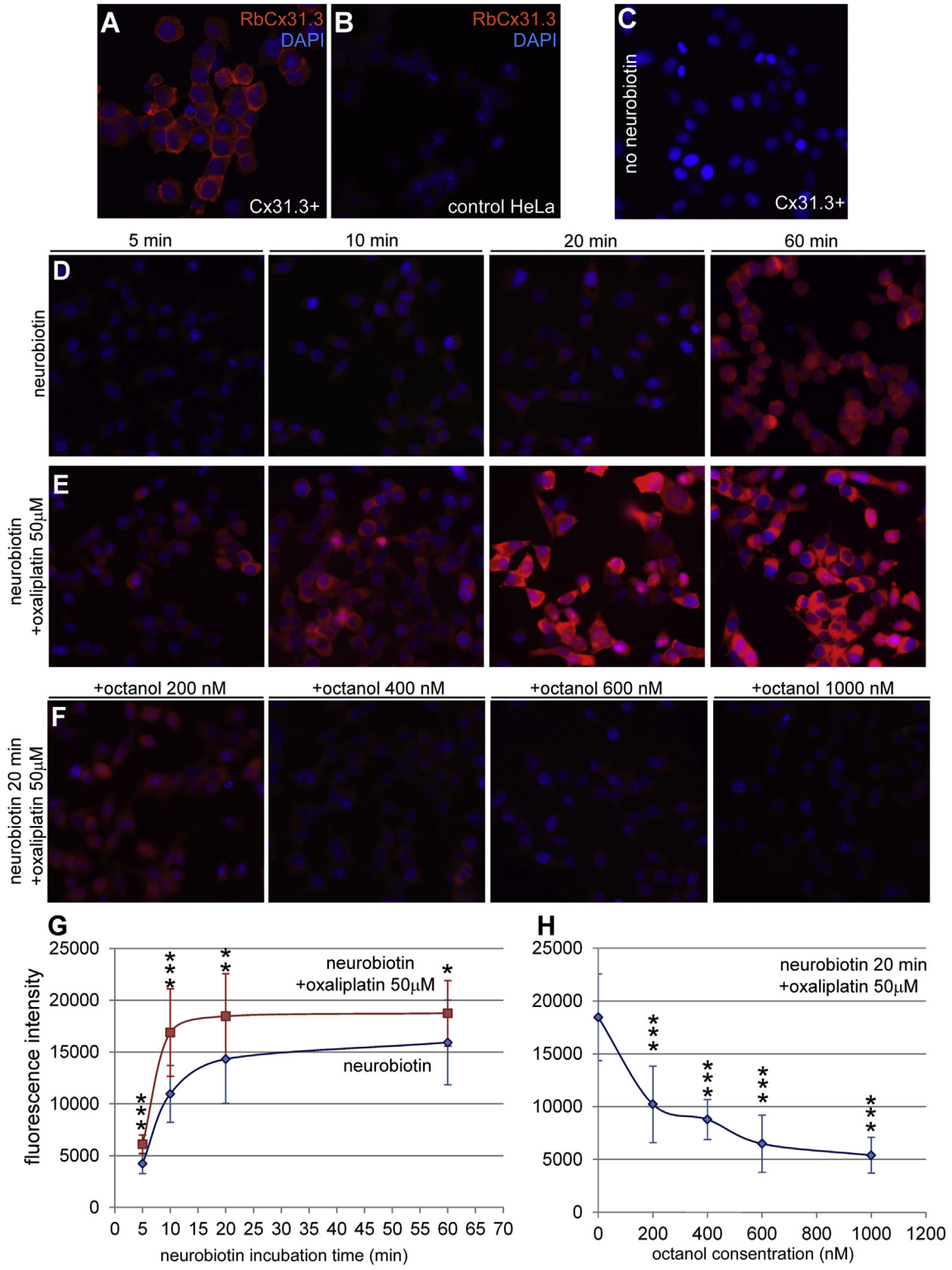

Fig. 9. Oxaliplatin accelerates Cx31.3 hemichannel opening and this effect is blocked by octanol in a dose-dependent manner. Expression of Cx31.3 in clonal Hela cells on the cell surface was confirmed by immunostaining with specific anti-Cx31.3 antibody (A), in contrast to control HeLa cells showing no specific Cx31.3 immunoreactivity (B). Representative images of Cx31.3-expressing cells from different neurobiotin incubation times as indicated without (D) or with oxaliplatin preincubation (E) shows increased neurobiotin signal at all time points in oxaliplatin treated cells. Cx31.3 cells without neurobiotin incubation show no specific signal (C). Quantification from 3 independent experiments (G) shows significantly higher neurobiotin uptake at all time points in oxaliplatin treated cells. Accelerated uptake in the presence of oxaliplatin is most pronounced at earlier intervals and reaches a plateau within 20 min, while in the absence of oxaliplatin the plateau is reached after 60 min. F: Exposure of Cx31.3 cells to combination of oxaliplatin and increasing concentrations of octanol for 20 min shows that the effect of oxaliplatin is blocked by octanol in a dose-depended manner. Quantification of neurobiotin signal (H) confirms the significant antagonism of the oxaliplatin effect by increasing octanol concentrations. *: $P < 0.05$; **: $P < 0.01$; ***: $P < 0.001$.

Since OIN appears to also involve even more prominently the GJ channels formed by Cx32 in myelinated fibers, we also examined *in vitro* the effect of oxaliplatin in cultured cells expressing the human Cx32. In order to assess Cx32 GJ channel function, we used the neurobiotin scrape loading assay. The addition of 25 μM oxaliplatin resulted in accelerated dye coupling between cells after 15 min compared to baseline dye coupling ($p < 0.05$). This effect of oxaliplatin was blocked by co-administration of octanol 400 nM (Supplementary Fig. 1). Thus, oxaliplatin appears to also cause opening of Cx32 GJ channels.

4. Discussion

Peripheral neuropathy remains the main dose-limiting toxicity of oxaliplatin in the majority of treated patients (Kweekel et al., 2005; Park et al., 2009). The clarification of the cellular mechanisms underlying OIN in the peripheral nervous system and identification of a successful neuroprotective strategy could have a major impact on improving patient quality of life and the ability to deliver full doses of oxaliplatin. Using the *ex vivo* preparation based on the isolated sciatic nerve of the mouse, we first examined separately the functional effects of octanol, a GJ blocker, and oxaliplatin on the sciatic nerve fibers and then in co-application. Our work was combined with morphological and *in vitro* studies, to demonstrate the neuroprotective properties of octanol. Our study implicates both Cx32 GJ channels and Cx29/Cx31.3 hemichannels in OIN and demonstrates that the co-administration of the GJ blocker octanol can prevent the effects of oxaliplatin on peripheral nerve myelinated fibers. Octanol appears to offer the best therapeutic window compared to three other GJ blockers tested, which showed weaker neuroprotective effects and more toxicity. Furthermore, we provide an explanation for the origin of hyperexcitability in acute OIN, as well as a structural correlate for the chronic manifestations.

The main advantage of our study is the use of the *ex vivo* preparation of the isolated mouse sciatic nerve, which provides stable in amplitude and duration recordings from either WT, Cx32 KO and Cx29 KO animals for at least 20 h. The long vitality of all three types of nerves in saline allowed us to perform long-term neuropharmacological experiments using a relatively low concentration of either octanol 200–600 nM, or oxaliplatin 25 μM. The concentration of oxaliplatin used in this study was only slightly above the concentrations used in clinical practice where after a dose of 130 mg/m^2 infused over 2 h, the plasma platinum mean C_{max} values were in the range of 2.59–3.22 μg/ml corresponding to 6.5–8.11 μM (Graham et al., 2000) or 3–6 μg/ml (8–16 μM) (Eckel et al., 2002). Moreover, the same oxaliplatin-effect was demonstrated in our previous *ex vivo* experiments even with a much lower concentration of 5 μM (Kagiava et al., 2008), but with a delay of 15–20 h. Therefore, we used here the concentration of 25 μM in order to provide clinical relevance to our *ex vivo* experiments (Kern et al., 1999), but also to have the oxaliplatin-effect developed within the time frame when the nerve preparation is still in perfect functional condition. In contrast, previous studies using similar nerve exposure models applied oxaliplatin 75–500 μM in order to achieve effects within 10–20 min (Adelsberger et al., 2000; Grolleau et al., 2001; Webster et al., 2005; Scuteri et al., 2010), an unusually high concentration which could have multiple effects on myelinated nerve fibers that may not be clinically relevant.

4.1. The effects of octanol on sciatic nerve GJs and GJ hemichannels

Octanol is a well-known GJ and GJ hemichannel blocker (Verselis and Srinivas, 2013), but has also been reported at higher concentrations to act as a blocker of Nav channels with an IC_{50} of 75 μM (Horishita and Harris, 2008) or even 455 μM (Poyraz et al., 2003). Here, octanol was tested against GJ and GJ hemichannels of myelinated nerve fibers at a much lower concentration of 200 and 400 nM causing an inhibition-recovery effect on the CAP amplitude, the octanol-effect, while at higher concentration over 600 nM it became neurotoxic, eliminating completely the amplitude of the CAP within 1 h at 2000 nM. The rapid decrease of the CAP amplitude indicates a fast loss of active nerve fibers. Interestingly, the strong inhibition of the CAP amplitude by octanol at such low concentrations confirms that GJs and GJ hemichannels located on the myelin sheath play a significant role in the generation and propagation of the action potential. These effects of octanol indicate that Cx29 and Cx32 play the main role in the homeostasis of K^+ in the periaxonal space at juxtaparanodes and juxtaincisures. The possible action of octanol against VGNaCs has already been excluded.

Cx29 hemichannels are located in the juxtaparanodal region in close proximity to the VGKCs and they provide a direct communication pathway between the periaxonal juxtaparanodal space and the Schwann cell, suggesting a close functional relationship (Altevogt et al., 2002). On the other hand, Cx32 forms GJs through the layers of non-compact myelin at paranodal loops and Schmidt–Lantermann incisures (Scherer et al., 1995) and plays an even more important role in the homeostasis of myelinated fibers and for preserving homeostasis in the periaxonal space (Anzini et al., 1997; Balice-Gordon et al., 1998; Sargiannidou et al., 2009; Vavlitou et al., 2010; Kleopa, 2011). Cx32 is required for normal function in peripheral nerves, as also demonstrated by the progressive neuropathy occurring in Cx32 KO mice (Anzini et al., 1997; Scherer et al., 1998; Sargiannidou et al., 2009; Vavlitou et al., 2010), as well as by the human disorders associated with Cx32 dysfunction (Kleopa, 2011). In contrast, Cx29 appears to play a less important role, since Cx29 KO mice show no morphological or basic electrophysiological abnormalities in the PNS or CNS (Eiberger et al., 2006) except for auditory neuropathy in 50% of cases (Tang et al., 2006).

4.2. The role of myelin GJ channels and hemichannels in K^+ spatial buffering

GJs and GJ hemichannels appear to play a crucial role in extracellular K^+ buffering at juxtaparanodes and periaxonal space, since blocking by octanol at 600–2000 nM in this study caused cancellation of the action potentials and eventually the loss of CAP, likely resulting from excess K^+ in the periaxonal space causing the malfunction of VGKCs. Others have similarly shown that the extra K^+ can modify membrane excitability (Kume-Kick et al., 2002) and even lead to hyperexcitation of myelinated nerve fibers (Chiu, 1991; Lev-Ram and Ellisman, 1995). Rapid clearance of K^+ from the juxtaparanodal periaxonal space is essential because during repetitive action potentials K^+ released by VGKCs in this very narrow space may reach concentrations of over 60 mM due to a very small distribution volume (Astion et al., 1988).

Based on our results of octanol interaction with GJ and GJ hemichannels and the known location and functional role of VGKCs in myelinated fibers (Konishi, 1990; Chiu, 1991), we propose the following siphoning mechanism by which GJ and GJ hemichannels may regulate the outflow of excess K^+ from the juxtaparanodal region, which is also in keeping with previous studies (Altevogt et al., 2002; Menichella et al., 2006): during an action potential the depolarization caused by the nodal Na^+ current activates both axonal Kv1.1/Kv1.2 and apposing GJ hemichannels so that they open almost simultaneously, or with a minor delay, the GJ hemichannels preceding the VGKCs. Almost all types of GJ hemichannels are activated (open) upon axon depolarization and are effectively closed by hyperpolarization (Paul et al., 1991; Valiunas and

Weingart, 2000; Kang et al., 2008; Fasciani et al., 2013) allowing substantial cation fluxes (Trexler et al., 1996). During this synchronized opening Kv1.1/Kv1.2 deliver K^+ into the narrow juxtaparanodal periaxonal space, Cx29 GJ hemichannels transfer the excess K^+ into the adaxonal Schwann cell cytoplasm, and from there it is further transported through the radial pathway formed by Cx32 GJs to the abaxonal Schwann cell cytoplasm. This flow results from accumulation of K^+ charging positively the juxtaparanodal periaxonal space combined with the negative Schwann cell membrane potential, near −40 mV (Hargittai et al., 1991). This brief influx of K^+ into the Schwann cell through the open hemichannels and GJ channels following electrical gradients lasts for a few milliseconds and stops at the end of action potential. Cx29 GJ hemichannels are the only known channels apposing juxtaparanodal axonal VGKCs (Altevogt et al., 2002), whereas Cx32 GJs are concentrated in the surrounding non-compact myelin areas (Scherer et al., 1995; Kleopa, 2011). Other channel types such as Kir2.1 and Kir2.3 are located at the microvilli surrounding the nodes of Ranvier (Mi et al., 1996) and may buffer extracellular K^+ at the node, while Schwann cells may transport excess K^+ from the cytoplasm to the capillaries through other channels facing the basilar membrane, including Kv1.5 (Horio, 2001).

4.3. The oxaliplatin effect

The functional correlate of OIN in the sciatic nerve fibers of the mouse, as demonstrated here, consists of a characteristic severe, time and concentration-dependent broadening of the evoked CAP repolarising phase, an effect also observed in other similar *ex vivo* studies (Adelsberger et al., 2000; Grolleau et al., 2001; Webster et al., 2005; Kagiava et al., 2008, 2013). This broadening results from increased duration of the RT (by about 300–400% of control) demonstrated in the intra-axonally recorded evoked action potentials from rat nerve fibers exposed to oxaliplatin (Kagiava et al., 2013). This type of prolongation indicates a hyperexcitation of the nerve fibers but only during the evoked action potential, since their resting membrane potential remains constant, between −80 and −90 mV, for over 1 h incubation in oxaliplatin (Kagiava et al., 2013). Our previous work (Kagiava et al., 2008) has shown that this unusual hyperexcitation caused by oxaliplatin in rat nerve fibers is closely related to the malfunction of VGKCs (Vabnick et al., 1999; Rasband et al., 2002). Interestingly, peripheral nerve fiber hyperexcitability that develops acutely following oxaliplatin exposure resembles neuromyotonia, a channelopathy linked to dysfunction of juxtaparanodal VGKCs (Hart et al., 2002; Kleopa et al., 2006; Van Poucke et al., 2012). Furthermore, the effects blocking VGKCs with 4-AP in nerve fibers from young animals before completed myelination (Astion et al., 1988) had a striking similarity with the recordings obtained after oxaliplatin treatment in adult nerve fibers (Kagiava et al., 2013), a clear indication of VGKCs malfunction during this unusual hyperexcitability developing only during the action potential. However, in contrast to 4-AP, direct binding of oxaliplatin to juxtaparanodal Kv1.1/1.2 VGKCs could not be confirmed (Adelsberger et al., 2000; Broomand et al., 2009) suggesting that VGKC involvement in OIN is likely through a functionally related target.

The severe broadening of RT of the evoked CAP by 25 μM oxaliplatin, found in all nerves examined, could be interpreted as a direct distortion of VGKCs, causing increase of K^+ in the fiber. However, this is not the case since the whole oxaliplatin-effect was reversed by 88.6% though octanol, a well-known blocker of GJ channels and hemichannels. This a clear indication that the malfunction of VGKCs during the oxaliplatin-effect is secondary to dysfunction of GJ and GJ hemichannels Thus, the conclusion is that oxaliplatin acts as an opener of GJ channels and hemichannels, causing a state of prolonged opening as also reported in other pathological conditions (Contreras et al., 2003; Gomes et al., 2005; Retamal et al., 2007; Orellana et al., 2010).

In order to clarify whether octanol acts on full GJs formed by Cx32 (Scherer et al., 1995) or on GJ hemichannels formed by Cx29 (Altevogt et al., 2002), the only known connexin channels in peripheral nerves, or both, we further investigated its effects in Cx32 KO and Cx29 KO mice. The vitality of the KO nerves was not significantly affected by the recording conditions although Cx32 and Cx29 are important for myelinated nerve fiber function (Altevogt et al., 2002; Scherer et al., 1995). This is probably due to low frequency stimulation (1 Hz), which allows the remaining GJs or GJ hemichannels to maintain adequate homeostasis. KO nerves also responded to 400 nM octanol as the WT nerves. A difference was seen in the response to oxaliplatin, which was almost identical for Cx29 KO and WT (RT>1035%), but lower (683.9%) for the Cx32 KO. Shorter RT in the Cx32 KO CAP could be due to the absence of the second peak of the CAP waveform, observed in both WT and Cx29. Also, there was a significant difference in the response to prolonged exposure to oxaliplatin, during which in WT nerves RT increase persisted for over 1200 min while in the KO nerves there was a peak near 240–340 min and then the RT gradually decreased. Finally, the protection by octanol against the oxaliplatin-effect persisted in both connexin KO nerves, although with lower intensity in Cx32 KO than in Cx29 KO. Taken together, these results support our conclusion that oxaliplatin acts as an opener of GJ channels more than hemichannels in peripheral nerve fibers.

Prolonged or even permanent GJ channel and hemichannel opening in the presence of oxaliplatin would first prevent the removal of the excess K^+ caused by the activation of VGKCs and then permit passive, non-physiological K^+ transport from the Schwann cell cytoplasm to the juxtaparanodal periaxonal space following concentration gradients, gradually building a surplus of K^+ in this region. Disruption of K^+ homoeostasis by oxaliplatin with increased extracellular K^+ in the juxtaparanodal region is expected to affect VGKC function, explaining the increase of 400% in the repolarising phase of the action potential (Kagiava et al., 2013) and eventually the increase in the RT of the CAP shown here. The axon responds to this excess of extracellular K^+ by post-stimulus repetitive firing, which increases in frequency with time of exposure to oxaliplatin (Kagiava et al., 2013). This repetitive firing starts when repolarizing of the action potential reaches values near −48 to −50 mV, the activation level of the fast Kv channels (Baker and Ritchie, 1996), and ends near the normal resting membrane potential of −90 mV (Kagiava et al., 2013). This has been suggested to act as a pumping mechanism for the release of the excess K^+ from the axon to the periaxonal juxtaparanodal region (Kagiava et al., 2013). Such a repetitive firing has also been observed in rat nerve fibers exposed to 4-AP (Astion et al., 1988) or even in the CNS of the locust, where pharmacological blockade of GJs induces repetitive surging of extracellular K^+. Thus, glial spatial buffering through GJs plays an essential role in the regulation of $[K^+]$ under normal conditions, contributing to K^+ clearance following physiologically elevated levels (Rash, 2010; Spong and Robertson, 2013). These phenomena are clinically relevant, as in oxaliplatin treated patients nerve conduction studies reveal hyperexcitability which appears as repetitive motor discharges after single electrical stimulus (Wilson et al., 2002; Lehky et al., 2004), while sensory hyperexcitability findings precede the development of neuropathy (Park et al., 2009). Why cold induces paresthesias in acute OIN (Lehky et al., 2004) remains unclear, but this phenomenon may be related to the fact that cold impairs GJ conductance as well as biosynthesis (Bukauskas and Weingart, 1993; Saitongdee et al., 2000), so that GJ channels may be more vulnerable to the effects of oxaliplatin at

lower temperatures. Further experimental insights will be needed to clarify the role of temperature in OIN.

4.4. Neuroprotection of octanol against oxaliplatin

Octanol when applied simultaneously with oxaliplatin compensated for the opening of GJ channels and hemichannels by oxaliplatin rescuing the prolongation of the CAP repolarising time from 1173.8 ± 0.92% of baseline when oxaliplatin was applied alone to only 146.0 ± 13.29% even after 1200 min incubation, an 88.6% protection. Indeed, the neuroprotection offered by octanol was slightly concentration-dependent with a minimum at 200 nM (85.3% protection of RT prolongation) and a maximum at 600 nM (87.7% protection). Octanol offers almost the same neuroprotection at the low concentration of 200 nM as at the higher and neurotoxic 600 nM. This is clinically relevant because the minimum effective octanol concentration should be used, to minimize the side effect of decreasing the CAP amplitude and the number of malfunctioning nerve fibers. Furthermore, supporting its opposite action of GJ channels and hemichannel opening, oxaliplatin appeared to protect against the octanol-effect, the inhibition-recovery of CAP amplitude. In the presence of oxaliplatin and 400 nM octanol there was a 98% maximum recovery in the amplitude of CAP, instead of 67% when octanol was applied alone. The protective role of oxaliplatin became even more pronounced when applied simultaneously with 600 nM octanol, a concentration that proved to be neurotoxic for the nerve fibers when applied alone. With this combination the CAP recovered up to 90%, as opposed to complete loss in the presence of 600 nM octanol alone. This is a clear indication that the opening and fixation of GJ and GJ hemichannels by oxaliplatin is compensated by octanol.

These mutual neuroprotective effects occurred only when the two compounds were added simultaneously or when the nerve was pre-incubated in octanol. In contrast, when the nerve was pre-incubated in oxaliplatin and then in octanol the neuroprotective effect became neurotoxic. The reason for this phenomenon remains unclear, but may be related to the nature of interaction of each compound with the connexins channels, that could involve common or different binding sites and cause conformational changes of channel forming domains (Spray et al., 1986) affecting the subsequent binding of the other compound. Octanol, similar to other GJ blockers, has been shown to bind only to extracellular connexin sites that differ from the Ca^{2+} binding site (Eskandari et al., 2002), while the biophysical interaction of oxaliplatin with connexins will need to be clarified in future studies. A similar effect was reported in other models where connexin hemichannel blockade was neuroprotective after, but not during global cerebral ischemia in near-term fetal sheep (Davidson et al., 2014). The neuroprotective role of octanol against oxaliplatin found in the sciatic nerve preparation was verified by our *in vitro* experiments in HeLa cells expressing Cx31.3, the human ortholog of Cx29 (Sargiannidou et al., 2008), where oxaliplatin accelerated the uptake of neurobiotin through hemichannels but this opening effect was reversed by octanol in a concentration-dependent manner. Furthermore, oxaliplatin accelerated dye transfer between Cx32 expressing cells, and this effect was again reversed by octanol.

Thus, oxaliplatin appears to uncouple and maintain open Cx32 channels and Cx29 hemichannels that would normally open only briefly during the passage of action potential, canceling the K^+ siphoning mechanism. Excess extracellular K^+ in the narrow juxtaparanodal region disrupts VGKC function and this appears in the post-stimulus intra-axonal action potential as either a plateau or as repetitive firing (Kagiava et al., 2013). This gradual juxtaparanodal accumulation of K^+ increasingly affecting VGKC function would explain why the oxaliplatin-effect in this study and in all our previous experiments performed in rodent nerves using similar oxaliplatin concentrations (Kagiava et al., 2008, 2013) occurs with a delay, which is time- and concentration-dependent. In our experiment with 25 μM oxaliplatin the development of the maximum oxaliplatin-effect occurred within 300–360 min in nerves from either WT or KO animals. At higher concentrations, 150 μM oxaliplatin, the same effect occurred within 50–60 min (Kagiava et al., 2013). The model of oxaliplatin-induced uncoupling of connexin channels proposed here for the peripheral nerve could also explain in part the increased coupling of satellite cells in DRGs induced by oxaliplatin, lowering pain threshold, which can also be antagonized by GJ blockers (Warwick and Hanani, 2013), as well as the increased coupling of spinal cord astrocytes leading to oxaliplatin-induced mechanical hypersensitivity (Yoon et al., 2013).

4.5. Morphological changes following prolonged oxaliplatin exposure

Our electrophysiological studies show that nerve fibers incubated in 25 μM oxaliplatin develop within the first 3–4 h a severe increase in the RT of the CAP which reaches a maximum and persists for the remaining of the 20 h incubation time. We then asked whether there is an ultrastructural correlate to this oxaliplatin effect. Detailed morphological studies revealed that after the first 300 min, when the electrophysiological alterations are fully developed, there is no alteration in the fine structure of the nerve fibers, focusing on perinodal areas. Thus, functional alterations in our model precede any morphological changes, as also described in the clinical setting (Lehky et al., 2004; Park et al., 2009). This fact also excludes the possibility that oxaliplatin causes a primary structural alteration or redistribution of VGKCs and associated molecules or Cx29 hemichannels, that could then lead to dysfunction of the peripheral nerve. However, with further oxaliplatin exposure for 1200 min we found characteristic axonal edema in the juxtaparanodal areas, as shown by teased fiber and electron microscopy examination. These changes occurred only in oxaliplatin treated fibers that exhibited the CAP prolongation, but not in control or in oxaliplatin + octanol treated fibers, again in line with clinical data supporting that the early findings of hyperexcitability are predictive of later development of neuropathy (Park et al., 2009).

Despite the late morphological changes in the juxtaparanodal areas due to axonal edema, the clustering of VGKCs in oxaliplatin-exposed nerves was not disrupted (Poliak et al., 2003; Traka et al., 2003), nor there was any diffusion of VGKCs into the paranodal areas (Boyle et al., 2001) as seen in mutants of axonal domains. Furthermore, none of those mutants show the severe CAP prolongation caused by oxaliplatin. Finally, we could not detect any abnormalities in Na^+/K^+ ATPase subunit expression, in agreement with previous electrophysiological studies showing a much different functional effect of ATPase blockers on the sciatic nerve compared to the oxaliplatin effect (Kagiava et al., 2012), indicating that ATPase is not directly involved in OIN.

The edematous axonal changes following prolonged oxaliplatin exposure are unique. We speculate that prolonged nerve exposure to oxaliplatin and as a result the uncoupling and persistent opening of Cx29 hemichannels and Cx32 GJs in the myelin sheath leads to reversal of K^+ flow from Schwann cell cytoplasm to the periaxonal space. Gradual accumulation of K^+ in this narrow space and cancellation of the activity-dependent siphoning function (above) may also reverse cation flow resulting in osmotic edema in the axon. Similar mechanisms have been described in the CNS (Rash, 2010), where the collapse of K^+ homeostasis may lead to disruption of the resting membrane potential, release of cytotoxic levels of

ATP (Kang et al., 2008) and uptake of water resulting in cell swelling and rupture (Quist et al., 2000).

4.6. Octanol as neuroprotectant against OIN in clinical practice

Numerous attempts to reduce OIN have been reported, using goshajinkigan (Ushio et al., 2012), synthetic eel calcitonin and elcatonin (Aoki et al., 2012), neurotropin (Kawashiri et al., 2011), silibinin (Di Cesare Mannelli et al., 2012), minocycline (Boyette-Davis and Dougherty, 2011), monosialotetrahexosyl ganglioside (Chen et al., 2012), and calcium blockers (Tatsushima et al., 2013). Similarly, ethosuximide (Flatters and Bennett, 2004) and neurotropin (Kawashiri et al., 2009) were found to reverse paclitaxel-induced peripheral neuropathy without affecting anti-tumor efficacy. This study clearly supports the potential for octanol to efficiently prevent OIN by blocking Cx32 and Cx29 channels, which are present in rodent peripheral nerves. This protective effect was verified by our *in vitro* experiments in HeLa cells expressing either of the two connexins. Thus, octanol can be used for medical treatment since it was found to be well-tolerated and safe in clinical trials for essential tremor (Bushara et al., 2004; Haubenberger et al., 2014). The optimal administration protocol will have to be developed, since for maximum protection we had to apply the two compounds, octanol and oxaliplatin simultaneously. Nevertheless, administration of octanol prior to oxaliplatin still provided a marked neuroprotection. Octanol offers the advantage that it can be used at very low concentrations (200 nM) against OIN, while for other blockers such as GRA much higher concentrations (25 μM) are required to offer a weaker protection. Although octanol offers almost the same neuroprotection against OIN at low and high concentrations, the lower concentrations appear to have almost no side effects, reflected in CAP preservation. Further studies in *in vivo* models of OIN will be needed to reproduce the *ex vivo* findings and inform the best approach for future clinical trials as well.

Besides octanol we also studied three more GJ blockers, carbenoxolone, GRA and OA for the potential to offer protection against OIN. Overall, they provided weaker or no protection at lower concentrations, over 125–1500 times higher than the corresponding concentration for octanol, with little toxicity, whereas at higher concentrations they were neurotoxic, eliminating the CAP. Thus, carbenoxolone offered no protective effect at non-toxic concentrations (25 μM), while OA (300 μM) offered only a 37.6% improvement in RT prolongation caused by oxaliplatin. GRA (25 μM) showed a better profile, offering a clear neuroprotective effect of 78.8% at relatively non-toxic concentrations. Thus, GRA largely reproduced the effects of octanol, but at much higher concentrations. Furthermore, oxaliplatin antagonized the negative impact of GRA on the CAP, as we observed for octanol. This high concentration may be deleterious when used in *in vivo* studies or in clinical practice. The lack of protection by carbenoxolone may be due to the fact that it has a number of other effects, including a reduction in excitatory and inhibitory synaptic currents, alteration of intrinsic membrane properties and suppression of action potentials (Rouach et al., 2003; Tovar et al., 2009; Beaumont and Maccaferri, 2011). Carbenoxolone has also been reported to block Ca^{2+} channels, pannexin channels and P2X7 receptors at concentrations similar to or lower than those blocking connexin channels (Vessey et al., 2004; Bruzzone et al., 2005; Suadicani et al., 2006). Taken together, the results of testing further GJ blockers against OIN confirm the protective effect of blocking GJ channels. However, octanol remains the best choice with the most favorable therapeutic window.

In **conclusion**, we provide a mechanistic explanation for OIN based on uncoupling by oxaliplatin of Cx32 GJ channels and Cx29/Cx31.3 hemichannels apposing VGKCs, leading to early functional abnormalities promoting hyperexcitability, and to later morphological changes consisting of axonal juxtaparanodal edema. Furthermore, the clinically relevant GJ blocker octanol effectively prevents oxaliplatin effects *ex vivo* and *in vitro* and should be further studied for the possibility of preventive use in OIN.

Acknowledgments

This work was funded in part by the Cyprus Telethon (2006–2014), the Muscular Dystrophy Association (Grant MDA 277250) and the European Leukodystrophy Association (ELA 2011-025I2). We would like to thank Marianna Nearchou for assistance with processing EM samples and Styliana Kyriakoudi for help with in vitro experiments. The ATPase-a1 antibody developed by D.M. Fambrough was obtained from the Developmental Studies Hybridoma Bank developed under the auspices of the NICHD and maintained by the University of Iowa, Department of Biological Sciences, Iowa, City, IA 52242.

Appendix A. Supplementary data

Supplementary data related to this article can be found at http://dx.doi.org/10.1016/j.neuropharm.2015.05.021.

References

Adelsberger, H., Quasthoff, S., Grosskreutz, J., Lepier, A., Eckel, F., Lersch, C., 2000. The chemotherapeutic oxaliplatin alters voltage-gated Na(+) channel kinetics on rat sensory neurons. Eur. J. Pharmacol. 406, 25–32.

Altevogt, B.M., Kleopa, K.A., Postma, F.R., Scherer, S.S., Paul, D.L., 2002. Connexin29 is uniquely distributed within myelinating glial cells of the central and peripheral nervous systems. J. Neurosci. 22, 6458–6470.

Andre, T., Boni, C., Mounedji-Boudiaf, L., Navarro, M., Tabernero, J., Hickish, T., Topham, C., Zaninelli, M., Clingan, P., Bridgewater, J., Tabah-Fisch, I., de Gramont, A., Multicenter International Study of Oxaliplatin/5-Fluorouracil/Leucovorin in the Adjuvant Treatment of Colon Cancer I, 2004. Oxaliplatin, fluorouracil, and leucovorin as adjuvant treatment for colon cancer. N. Engl. J. Med. 350, 2343–2351.

Anzini, P., Neuberg, D.H.-H., Schachner, M., Nelles, E., Willecke, K., Zielasek, J., Toyka, K., Suter, U., Martini, R., 1997. Structural abnormalities and deficient maintenance of peripheral nerve myelin in mice lacking the gap junction protein connexin32. J. Neurosci. 17, 4545–4561.

Aoki, M., Mori, A., Nakahara, T., Sakamoto, K., Ishii, K., 2012. Effect of synthetic eel calcitonin, elcatonin, on cold and mechanical allodynia induced by oxaliplatin and paclitaxel in rats. Eur. J. Pharmacol. 696, 62–69.

Argyriou, A.A., Cavaletti, G., Antonacopoulou, A., Genazzani, A.A., Briani, C., Bruna, J., Terrazzino, S., Velasco, R., Alberti, P., Campagnolo, M., Lonardi, S., Cortinovis, D., Cazzaniga, M., Santos, C., Psaromyalou, A., Angelopoulou, A., Kalofonos, H.P., 2013. Voltage-gated sodium channel polymorphisms play a pivotal role in the development of oxaliplatin-induced peripheral neurotoxicity: results from a prospective multicenter study. Cancer 119, 3570–3577.

Astion, M.L., Coles, J.A., Orkand, R.K., Abbott, N.J., 1988. K^+ accumulation in the space between giant axon and Schwann cell in the squid Alloteuthis. Effects of changes in osmolarity. Biophys. J. 53, 281–285.

Baker, M.D., Ritchie, J.M., 1996. Characteristics of type I and type II K^+ channels in rabbit cultured Schwann cells. J. Physiol. 490, 79–95.

Balice-Gordon, R.J., Bone, L.J., Scherer, S.S., 1998. Functional gap junctions in the Schwann cell myelin sheath. J. Cell Biol. 142, 1095–1104.

Beaumont, M., Maccaferri, G., 2011. Is connexin36 critical for GABAergic hypersynchronization in the hippocampus? J. Physiol. 589, 1663–1680.

Benoit, E., Brienza, S., Dubois, J.M., 2006. Oxaliplatin, an anticancer agent that affects both Na^+ and K^+ channels in frog peripheral myelinated axons. Gen. Physiol. Biophys. 25, 263–276.

Boyette-Davis, J., Dougherty, P.M., 2011. Protection against oxaliplatin-induced mechanical hyperalgesia and intraepidermal nerve fiber loss by minocycline. Exp. Neurol. 229, 353–357.

Boyle, M.E.T., Berglund, E.O., Murai, K.K., Weber, L., Peles, E., Ranscht, B., 2001. Contactin orchestrates assembly of the septate-like junctions at the paranode in myelinated peripheral nerve. Neuron 30, 385–397.

Broomand, A., Jerremalm, E., Yachnin, J., Ehrsson, H., Elinder, F., 2009. Oxaliplatin neurotoxicity – no general ion channel surface-charge effect. J. Negat. Results Biomed. 8, 2.

Bruzzone, R., Barbe, M.T., Jakob, N.J., Monyer, H., 2005. Pharmacological properties of homomeric and heteromeric pannexin hemichannels expressed in *Xenopus oocytes*. J. Neurochem. 92, 1033–1043.

Bukauskas, F.F., Weingart, R., 1993. Temperature dependence of gap junction properties in neonatal rat heart cells. Pflug. Arch. 423, 133–139.

Burakgazi, A.Z., Messersmith, W., Vaidya, D., Hauer, P., Hoke, A., Polydefkis, M., 2011. Longitudinal assessment of oxaliplatin-induced neuropathy. Neurology 77, 980–986.
Bushara, K.O., Goldstein, S.R., Grimes Jr., G.J., Burstein, A.H., Hallett, M., 2004. Pilot trial of 1-octanol in essential tremor. Neurology 62, 122–124.
Chen, X.F., Wang, R., Yin, Y.M., Roe, O.D., Li, J., Zhu, L.J., Guo, R.H., Wu, T., Shu, Y.Q., 2012. The effect of monosialotetrahexosylganglioside (GM1) in prevention of oxaliplatin induced neurotoxicity: a retrospective study. Biomed. Pharmacother. 66, 279–284.
Chiu, S.Y., 1991. Functions and distribution of voltage-gated sodium and potassium channels in mammalian Schwann cells. Glia 4, 541–558.
Contreras, J.E., Sáez, J.C., Bukauskas, F.F., Bennett, M.V., 2003. Gating and regulation of connexin 43 (Cx43) hemichannels. Proc. Natl. Acad. Sci. U. S. A. 100, 11388–11393.
Davidson, J.O., Drury, P.P., Green, C.R., Nicholson, L.F., Bennet, L., Gunn, A.J., 2014. Connexin hemichannel blockade is neuroprotective after asphyxia in preterm fetal sheep. PLoS One 9 (5), e96558.
Di Cesare Mannelli, L., Z, M., Failli, P., Ghelardini, C., 2012. Oxaliplatin-induced neuropathy: oxidative stress as pathological mechanism. Protective effect of silibinin. J. Pain 13, 276–284.
Dimitrov, A.G., Dimitrova, N.A., 2012. A possible link of oxaliplatin-induced neuropathy with potassium channel deficit. Muscle Nerve 45, 403–411.
Eckel, F., Schmelz, R., Adelsberger, H., Erdmann, J., Quasthoff, S., Lersch, C., 2002. Prevention of oxaliplatin-induced neuropathy by carbamazepine. A pilot study. Dtsch. Med. Wochenschr. 127, 78–82.
Eiberger, J., Kibschull, M., Strenzke, N., Schober, A., Büssow, H., Wessig, C., Djahed, S., Reucher, H., Koch, D.A., Lautermann, J., Moser, T., Winterhager, E., Willecke, K., 2006. Expression pattern and functional characterization of connexin29 in transgenic mice. Glia 53, 601–611.
Eskandari, S., Zampighi, G.A., Leung, D.W., Wright, E.M., Loo, D.D., 2002. Inhibition of gap junction hemichannels by chloride channel blockers. J. Membr. Biol. 185, 93–102.
Fasciani, I., Temperan, A., Perez-Atencio, L.F., Escudero, A., Martinez-Montero, P., Molano, J., Gomez-Hernandez, J.M., Paino, C.L., Gonzalez-Nieto, D., Barrio, L.C., 2013. Regulation of connexin hemichannel activity by membrane potential and the extracellular calcium in health and disease. Neuropharmacology 75, 479–490.
Ferrier, J., Pereira, V., Busserolles, J., Authier, N., Balayssac, D., 2013. Emerging trends in understanding chemotherapy-induced peripheral neuropathy. Curr. Pain Headache Rep. 17, 364.
Flatters, S.J., Bennett, G.J., 2004. Ethosuximide reverses paclitaxel- and vincristine-induced painful peripheral neuropathy. Pain 109, 150–161.
Gomes, P., Srinivas, S.P., Van Driessche, W., Vereecke, J., Himpens, B., 2005. ATP release through connexin hemichannels in corneal endothelial cells. Invest. Ophthalmol. Vis. Sci. 46, 1208–1218.
Graham, M.A., Lockwood, G.F., Greenslade, D., Brienza, S., Bayssas, M., Gamelin, E., 2000. Clinical pharmacokinetics of oxaliplatin: a critical review. Clin. Cancer Res. 6, 1205–1218.
Grolleau, F., Gamelin, L., Boisdron-Celle, M., Lapied, B., Pelhate, M., Gamelin, E., 2001. A possible explanation for a neurotoxic effect of the anticancer agent oxaliplatin on neuronal voltage-gated sodium channels. J. Neurophysiol. 85, 2293–2297.
Hargittai, P.T., Youmans, S.J., Lieberman, E.M., 1991. Determination of the membrane potential of cultured mammalian Schwann cells and its sensitivity to potassium using a thiocarbocyanine fluorescent dye. Glia 4, 611–616.
Hart, I.K., Maddison, P., Newsom-Davis, J., Vincent, A., Mills, K.R., 2002. Phenotypic variants of autoimmune peripheral nerve hyperexcitability. Brain 125, 1887–1895.
Haubenberger, D., Nahab, F.B., Voller, B., Hallet, M., 2014. Treatment of essential tremor with long-chain alcohols: still experimental or ready for prime time? Tremor Other Hyperkinetic Mov. http://dx.doi.org/10.7916/D8RX991R.
Hochster, H.S., Grothey, A., Childs, B.H., 2007. Use of calcium and magnesium salts to reduce oxaliplatin-related neurotoxicity. J. Clin. Oncol. 25, 4028–4029.
Horio, Y., 2001. Potassium channels of glial cells: distribution and function. Jpn. J. Pharmacol. 87, 1–6.
Horishita, T., Harris, R.A., 2008. n-Alcohols inhibit voltage-gated Na^+ channels expressed in *Xenopus oocytes*. J. Pharmacol. Exp. Ther. 326, 270–277.
Kagiava, A., Aligizaki, K., Katikou, P., Nikolaidis, G., Theophilidis, G., 2012. Assessing the neurotoxic effects of palytoxin and ouabain, both Na(+)/K(+)-ATPase inhibitors, on the myelinated sciatic nerve fibres of the mouse: an ex vivo electrophysiological study. Toxicon 59, 416–426.
Kagiava, A., Kosmidis, E.K., Theophilidis, G., 2013. Oxaliplatin-induced hyperexcitation of rat sciatic nerve fibers: an intra-axonal study. Anticancer Agents Med. Chem. 13, 373–379.
Kagiava, A., Tsingotjidou, A., Emmanouilides, C., Theophilidis, G., 2008. The effects of oxaliplatin, an anticancer drug, on potassium channels of the peripheral myelinated nerve fibres of the adult rat. Neurotoxicology 29, 1100–1106.
Kang, J., Kang, N., Lovatt, D., Torres, A., Zhao, Z., Lin, J., Nedergaard, M., 2008. Connexin 43 hemichannels are permeable to ATP. J. Neurosci. 28, 4702–4711.
Kawashiri, T., Egashira, N., Itoh, Y., Shimazoe, T., Ikegami, Y., Yano, T., Yoshimura, M., Oishi, R., 2009. Neurotropin reverses paclitaxel-induced neuropathy without affecting anti-tumour efficacy. Eur. J. Cancer 45, 154–163.
Kawashiri, T., Egashira, N., Watanabe, H., Ikegami, Y., Hirakawa, S., Mihara, Y., Yano, T., Ikesue, H., Oishi, R., 2011. Prevention of oxaliplatin-induced mechanical allodynia and neurodegeneration by neurotropin in the rat model. Eur. J. Pain 15, 344–350.
Kern, W., Braess, J., Bottger, B., Kaufmann, C.C., Hiddemann, W., Schleyer, E., 1999. Oxaliplatin pharmacokinetics during a four-hour infusion. Clin. Cancer Res. 5, 761–765.
Kleopa, K.A., 2011. The role of gap junctions in Charcot-Marie-Tooth disease. J. Neurosci. 31, 17753–17760.
Kleopa, K.A., Elman, L.B., Lang, B., Vincent, A., Scherer, S.S., 2006. Neuromyotonia and limbic encephalitis sera target mature Shaker-type K^+ channels: subunit specificity correlates with clinical manifestations. Brain 129, 1570–1584.
Kocsis, J.D., Eng, D.L., Gordon, T.R., Waxman, S.G., 1987. Functional differences between 4-aminopyridine and tetraethylammonium-sensitive potassium channels in myelinated axons. Neurosci. Lett. 75, 193–198.
Konishi, T., 1990. Voltage-gated potassium currents in myelinating Schwann cells in the mouse. J. Physiol. 431, 123–139.
Krishnan, A.V., Goldstein, D., Friedlander, M., Kiernan, M.C., 2006. Oxaliplatin and axonal Na^+ channel function in vivo. Clin. Cancer Res. 12, 4481–4484.
Krøigård, T., Schrøder, H.D., Qvortrup, C., Eckhoff, L., Pfeiffer, P., Gaist, D., Sindrup, S.H., 2014. Characterization and diagnostic evaluation of chronic polyneuropathies induced by oxaliplatin and docetaxel comparing skin biopsy to quantitative sensory testing and nerve conduction studies. Eur. J. Neurol. 21, 623–629.
Kume-Kick, J., Mazel, T., Vorisek, I., Hrabetova, S., Tao, L., Nicholson, C., 2002. Independence of extracellular tortuosity and volume fraction during osmotic challenge in rat neocortex. J. Physiol. 542, 515–527.
Kweekel, D.M., Gelderblom, H., Guchelaar, H.J., 2005. Pharmacology of oxaliplatin and the use of pharmacogenomics to individualize therapy. Cancer Treat. Rev. 31, 90–105.
Lang, P.M., Fleckenstein, J., Passmore, G.M., Brown, D.A., Grafe, P., 2008. Retigabine reduces the excitability of unmyelinated peripheral human axons. Neuropharmacology 54, 1271–1278.
Lehky, T.J., Leonard, G.D., Wilson, R.H., Grem, J.L., Floeter, M.K., 2004. Oxaliplatin-induced neurotoxicity: acute hyperexcitability and chronic neuropathy. Muscle Nerve 29, 387–392.
Lev-Ram, V., Ellisman, M.H., 1995. Axonal activation-induced calcium transients in myelinating Schwann cells, sources, and mechanisms. J. Neurosci. 15, 2628–2637.
Loprinzi, C.L., Qin, R., Dakhil, S.R., Fehrenbacher, L., Flynn, K.A., Atherton, P., Seisler, D., Qamar, R., Lewis, G.C., Grothey, A., 2014. Phase III randomized, placebo-controlled, double-blind study of intravenous calcium and magnesium to prevent oxaliplatin-induced sensory neurotoxicity (N08CB/Alliance). J. Clin. Oncol. 32, 997–1005.
Menichella, D.M., Majdan, M., Awatramani, R., Goodenough, D.A., Sirkowski, E., Scherer, S.S., Paul, D.L., 2006. Genetic and physiological evidence that oligodendrocyte gap junctions contribute to spatial buffering of potassium released during neuronal activity. J. Neurosci. 26, 10984–10991.
Mi, H., Deerinck, T.J., Jones, M., Ellisman, M.H., Schwarz, T.L., 1996. Inwardly rectifying K^+ channels that may participate in K^+ buffering are localized in microvilli of Schwann cells. J. Neurosci. 16, 2421–2429.
Nodera, H., Spieker, A., Sung, M., Rutkove, S., 2011. Neuroprotective effects of Kv7 channel agonist, retigabine, for cisplatin-induced peripheral neuropathy. Neurosci. Lett. 505, 223–227.
Orellana, J.A., Hernández, D.E., Ezan, P., Velarde, V., Bennett, M.V., Giaume, C., Sáez, J.C., 2010. Hypoxia in high glucose followed by reoxygenation in normal glucose reduces the viability of cortical astrocytes through increased permeability of connexin 43 hemichannels. Glia 58, 329–343.
Park, S.B., Lin, C.S., Krishnan, A.V., Goldstein, D., Friedlander, M.L., Kiernan, M.C., 2009. Oxaliplatin-induced neurotoxicity: changes in axonal excitability precede development of neuropathy. Brain 132, 2712–2723.
Park, S.B., Lin, C.S., Krishnan, A.V., Goldstein, D., Friedlander, M.L., Kiernan, M.C., 2011. Dose effects of oxaliplatin on persistent and transient Na^+ conductances and the development of neurotoxicity. PLoS One 6, e18469.
Paul, D.L., Ebihara, L., Takemoto, L.J., Swenson, K.I., Goodenough, D.A., 1991. Voltage gating and permeation in a gap junction hemichannel. J. Cell Biol. 115, 1077–1089.
Poliak, S., Salomon, D., Elhanany, H., Sabanay, H., Kiernan, B., Pevny, L., Stewart, C.L., Xu, X., Chiu, S.Y., Shrager, P., Furley, A.J., Peles, E., 2003. Juxtaparanodal clustering of Shaker-like K^+ channels in myelinated axons depends on Caspr2 and TAG-1. J. Cell Biol. 162, 1149–1160.
Poyraz, D., Bräu, M.E., Wotka, F., Puhlmann, B., Scholz, A.M., Hempelmann, G., Kox, W.J., Spies, C.D., 2003. Lidocaine and octanol have different modes of action at tetrodotoxin-resistant Na(+) channels of peripheral nerves. Anesth. Analg. 97, 1317–1324.
Quist, A.P., Rhee, S.K., Lin, H., Lal, R., 2000. Physiological role of gap-junctional hemichannels. Extracellular calcium-dependent isosmotic volume regulation. J. Cell Biol. 148, 1063–1074.
Rasband, M.N., Park, E.W., Zhen, D., Arbuckle, M.I., Poliak, S., Peles, E., Grant, S.G., Trimmer, J.S., 2002. Clustering of neuronal potassium channels is independent of their interaction with PSD-95. J. Cell Biol. 159, 663–672.
Rash, J.E., 2010. Molecular disruptions of the panglial syncytium block potassium siphoning and axonal saltatory conduction: pertinence to neuromyelitis optica and other demyelinating diseases of the central nervous system. Neuroscience 168, 982–1008.
Retamal, M.A., Froger, N., Palacios-Prado, N., Ezan, P., Saez, P.J., Saez, J.C., Giaume, C., 2007. Cx43 hemichannels and gap junction channels in astrocytes are regulated oppositely by proinflammatory cytokines released from activated microglia. J. Neurosci. 27, 13781–13792.

Rouach, N., Segal, M., Koulakoff, A., Giaume, C., Avignone, E., 2003. Carbenoxolone blockade of neuronal network activity in culture is not mediated by an action on gap junctions. J. Physiol. 553, 729–745.
Saitongdee, P., Milner, P., Becker, D.L., Knight, G.E., Burnstock, G., 2000. Increased connexin43 gap junction protein in hamster cardiomyocytes during cold acclimatization and hibernation. Cardiovasc. Res. 47, 108–115.
Sakurai, M., Egashira, N., Kawashiri, T., Yano, T., Ikesue, H., Oishi, R., 2009. Oxaliplatin-induced neuropathy in the rat: involvement of oxalate in cold hyperalgesia but not mechanical allodynia. Pain 147, 165–174.
Sargiannidou, I., Ahn, M., Enriquez, A.D., Peinado, A., Reynolds, R., Abrams, C., Scherer, S.S., Kleopa, K.A., 2008. Human oligodendrocytes express Cx31.3: function and interactions with Cx32 mutants. Neurobiol. Dis. 30, 221–233.
Sargiannidou, I., Vavlitou, N., Aristodemou, S., Hadjisavvas, A., Kyriacou, K., Scherer, S.S., Kleopa, K.A., 2009. Connexin32 mutations cause loss of function in Schwann cells and oligodendrocytes leading to PNS and CNS myelination defects. J. Neurosci. 29, 4748–4761.
Scherer, S.S., Deschenes, S.M., Xu, Y.T., Grinspan, J.B., Fischbeck, K.H., Paul, D.L., 1995. Connexin32 is a myelin-related protein in the PNS and CNS. J. Neurosci. 15, 8281–8294.
Scherer, S.S., Xu, Y.-T., Nelles, E., Fischbeck, K., Willecke, K., Bone, L.J., 1998. Connexin32-null mice develop a demyelinating peripheral neuropathy. Glia 24, 8–20.
Scuteri, A., Galimberti, A., Ravasi, M., Pasini, S., Donzelli, E., Cavaletti, G., Tredici, G., 2010. NGF protects dorsal root ganglion neurons from oxaliplatin by modulating JNK/Sapk and ERK1/2. Neurosci. Lett. 486, 141–145.
Sittl, R., Carr, R.W., Fleckenstein, J., Grafe, P., 2010. Enhancement of axonal potassium conductance reduces nerve hyperexcitability in an in vitro model of oxaliplatin-induced acute neuropathy. Neurotoxicology 31, 694–700.
Spong, K.E., Robertson, R.M., 2013. Pharmacological blockade of gap junctions induces repetitive surging of extracellular potassium within the locust CNS. J. Insect Physiol. 59, 1031–1040.
Spray, D.C., Saez, J.C., Brosius, D., Bennett, M.V., Hertzberg, E.L., 1986. Isolated liver gap junctions: gating of transjunctional currents is similar to that in intact pairs of rat hepatocytes. Proc. Natl. Acad. Sci. U. S. A. 83, 5494–5497.
Suadicani, S.O., Brosnan, C.F., Scemes, E., 2006. P2X7 receptors mediate ATP release and amplification of astrocytic intercellular $Ca2^{+}$ signaling. J. Neurosci. 26, 1378–1385.
Tang, W., Zhang, Y., Chang, Q., Ahmad, S., Dahlke, I., Yi, H., Chen, P., Paul, D.L., Lin, X., 2006. Connexin29 is highly expressed in cochlear Schwann cells, and it is required for the normal development and function of the auditory nerve of mice. J. Neurosci. 26, 1991–1999.
Tatsushima, Y., Egashira, N., Narishige, Y., Fukui, S., Kawashiri, T., Yamauchi, Y., Oishi, R., 2013. Calcium channel blockers reduce oxaliplatin-induced acute neuropathy: a retrospective study of 69 male patients receiving modified FOLFOX6 therapy. Biomed. Pharmacother. 67, 39–42.
Tovar, K.R., Maher, B.J., Westbrook, G.L., 2009. Direct actions of carbenoxolone on synaptic transmission and neuronal membrane properties. J. Neurophysiol. 102, 974–978.
Traka, M., Goutebroze, L., Denisenko, N., Bessa, M., Nifli, A., Havaki, S., Iwakura, Y., Fukamauchi, F., Watanabe, K., Soliven, B., Girault, J.A., Karagogeos, D., 2003. Association of TAG-1 with Caspr2 is essential for the molecular organization of juxtaparanodal regions of myelinated fibers. J. Cell Biol. 162, 1161–1172.
Trexler, E.B., Bennett, M.V., Bargiello, T.A., Verselis, V.K., 1996. Voltage gating and permeation in a gap junction hemichannel. Proc. Natl. Acad. Sci. U. S. A. 93, 5836–5841.
Ushio, S., Egashira, N., Sada, H., Kawashiri, T., Shirahama, M., Masuguchi, K., Oishi, R., 2012. Goshajinkigan reduces oxaliplatin-induced peripheral neuropathy without affecting anti-tumour efficacy in rodents. Eur. J. Cancer 48, 1407–1413.
Vabnick, I., Trimmer, J.S., Schwarz, T.L., Levinson, S.R., Risal, D., Shrager, P., 1999. Dynamic potassium channel distributions during axonal development prevent aberrant firing patterns. J. Neurosci. 19, 747–758.
Valiunas, V., Weingart, R., 2000. Electrical properties of gap junction hemichannels identified in transfected HeLa cells. Pflug. Arch. 440, 366–379.
Van Poucke, M., Vanhaesebrouck, A.E., Peelman, L.J., Van Ham, L., 2012. Experimental validation of in silico predicted KCNA1, KCNA2, KCNA6 and KCNQ2 genes for association studies of peripheral nerve hyperexcitability syndrome in Jack Russell Terriers. Neuromuscul. Disord. 22, 558–565.
Vavlitou, N., Sargiannidou, I., Markoullis, K., Kyriacou, K., Scherer, S.S., Kleopa, K.A., 2010. Axonal pathology precedes demyelination in a mouse model of X-linked demyelinating/type I Charcot-Marie Tooth neuropathy. J. Neuropathol. Exp. Neurol. 69, 945–958.
Verselis, V.K., Srinivas, M., 2013. Connexin channel modulators and their mechanisms of action. Neuropharmacology 75, 517–524.
Vessey, J.P., Lalonde, M.R., Mizan, H.A., Welch, N.C., Kelly, M.E., Barnes, S., 2004. Carbenoxolone inhibition of voltage-gated Ca channels and synaptic transmission in the retina. J. Neurophysiol. 92, 1252–1256.
von Delius, S., Eckel, F., Wagenpfeil, S., Mayr, M., Stock, K., Kullmann, F., Obermeier, F., Erdmann, J., Schmelz, R., Quasthoff, S., Adelsberger, H., Bredenkamp, R., Schmid, R.M., Lersch, C., 2007. Carbamazepine for prevention of oxaliplatin-related neurotoxicity in patients with advanced colorectal cancer: final results of a randomised, controlled, multicenter phase II study. Invest. New Drugs 25, 173–180.
Warwick, R.A., Hanani, M., 2013. The contribution of satellite glial cells to chemotherapy-induced neuropathic pain. Eur. J. Pain 17, 571–580.
Webster, R.G., Brain, K.L., Wilson, R.H., Grem, J.L., Vincent, A., 2005. Oxaliplatin induces hyperexcitability at motor and autonomic neuromuscular junctions through effects on voltage-gated sodium channels. Br. J. Pharmacol. 146, 1027–1039.
Wilson, R.H., Lehky, T., Thomas, R.R., Quinn, M.G., Floeter, M.K., Grem, J.L., 2002. Acute oxaliplatin-induced peripheral nerve hyperexcitability. J. Clin. Oncol. 20, 1767–1774.
Yoon, S.Y., Robinson, C.R., Zhang, H., Dougherty, P.M., 2013. Spinal astrocyte gap junctions contribute to oxaliplatin-induced mechanical hypersensitivity. J. Pain 14, 205–214.
Zhou, L., Messing, A., Chiu, S.Y., 1999. Determinants of excitability at transition zones in Kv1.1-deficient myelinated nerves. J. Neurosci. 19, 5768–5781.